

# High-resolution structural study on pyridin-3-yl ebselen and its *N*-methylated tosylate and iodide derivatives

Ruyi Xu, Thomas Fellowes and Jonathan M. White\*

School of Chemistry and BIO-21 Institute, University of Melbourne, Parkville, VIC 3010, Melbourne, Australia. \*Correspondence e-mail: whitejm@unimelb.edu.au

Received 17 October 2022

Accepted 3 January 2023

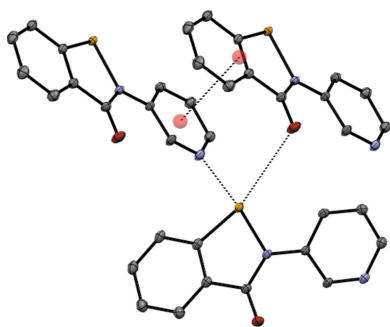
Edited by A. Peuronen, University of Sheffield, United Kingdom

**Keywords:** crystal structure; chalcogen bonding; hydrogen bonding; multipole refinement; electron density; ebselen; selenium.

**CCDC references:** 2234063; 2234062; 2234061; 2234060

**Supporting information:** this article has supporting information at journals.iucr.org/c

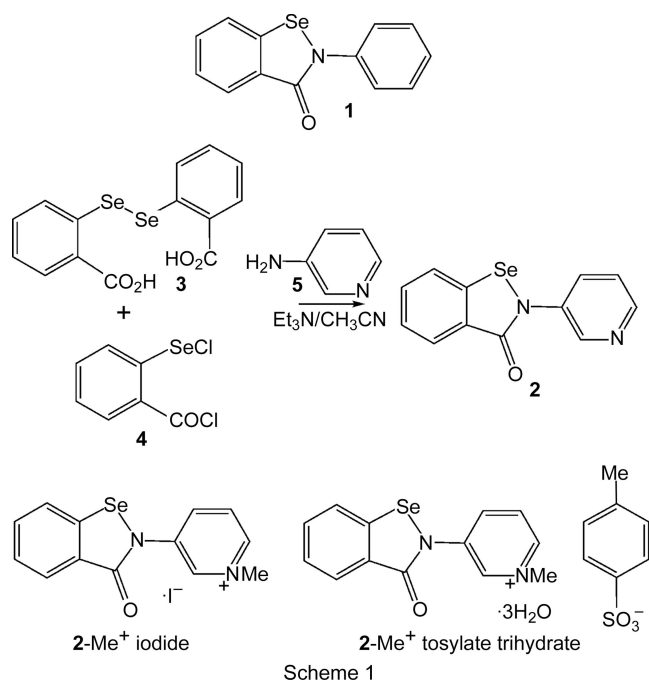
The crystal structure of the pyridine-substituted benzisoselenazolinone 2-(pyridin-3-yl)-2,3-dihydro-1,2-benzoselenazol-3-one ( $C_{12}H_8N_2OSe$ , **2**), related to the antioxidant ebselen [systematic name: 2-phenyl-1,2-benzoselenazol-3(2*H*)-one, **1**], is characterized by strong intermolecular  $N \cdots Se(-N)$  chalcogen bonding, where the  $N \cdots Se$  distance of 2.3831 (6) Å is well within the sum of the van der Waals radii for N and Se (3.34 Å). This strong interaction results in significant lengthening of the internal N—Se distance, consistent with significant population of the Se—N  $\sigma^*$  antibonding orbital. Much weaker intermolecular  $O \cdots Se$  chalcogen bonding occurs between the amide-like O atom in **2** and the less polarized C—Se bond in this structure. Charge density analysis of **2** using multipole refinement of high-resolution data allowed the electrostatic surface potential for **2** to be mapped, and clearly reveals the  $\sigma$ -hole at the extension of the Se—N bond as an area of positive electrostatic potential. Topological analysis of the electron-density distribution in **2** was carried out within the Quantum Theory of Atoms in Molecules (QTAIM) framework and revealed bond paths and (3,−1) bond critical points (BCPs) for the  $N \cdots Se-N$  moiety consistent with a closed-shell interaction; however, the potential energy term is suggestive of electron sharing. Analysis of the electron localization function (ELF) for the strong  $N \cdots Se$  and the weak  $O \cdots Se$  chalcogen-bonding interactions in the structure of **2** suggest significant electron sharing in the former interaction, and a largely electrostatic interaction in the latter. Conversion of **2** to its *N*-methylated derivatives by reaction with methyl iodide [1-methyl-3-(3-oxo-2,3-dihydro-1,2-benzoselenazol-2-yl)pyridin-1-ium iodide,  $C_{13}H_{11}N_2OSe^+ \cdot I^-$ ] and methyl tosylate [1-methyl-3-(3-oxo-2,3-dihydro-1,2-benzoselenazol-2-yl)pyridin-1-ium toluenesulfonate trihydrate,  $C_{13}H_{11}N_2OSe^+ \cdot C_7H_7O_3S^- \cdot 3H_2O$ ] removes the possibility of  $N \cdots Se$  chalcogen bonding and instead structures are obtained where the iodide and tosylate counter-ions fulfill the role of chalcogen-bond acceptors, with a strong  $I^- \cdots Se$  interaction in the iodide salt and a weaker  $p$ -Tol- $SO_3^- \cdots Se$  interaction in the tosylate salt.



## 1. Introduction

The benzisoselenazolinone scaffold of the drug ebselen (**1**) is a potent chalcogen-bond donor, due to the presence of a polarizable Se atom covalently bonded to an electron-withdrawing amide/aniline N atom. The propensity for this system to form chalcogen bonds has been studied within our group and by others, with a view to exploiting it in the context of medicinal chemistry (Thomas *et al.*, 2015; Fellowes & White, 2019; Fellowes *et al.*, 2020, 2022). However, the concept of chalcogen bonding has also received much attention concerning applications in materials chemistry (Eckstein *et al.*, 2021). In addition to the chalcogen-bond donor, ebselen also contains an amide carbonyl group which nicely fulfils the role of chalcogen-bond acceptor in directing the crystal packing of

this molecule, forming one-dimensional polymers in both polymorphic modifications (Fig. 1) (Thomas *et al.*, 2015), held together by  $\text{Se} \cdots \text{O}=\text{C}$  chalcogen-bond interactions, with the  $\text{Se} \cdots \text{O}=\text{C}$  distances of 2.522 (1) and 2.533 (1) Å being well within the sum of the van der Waals radii for Se and O (3.41 Å) (Bondi, 1964). The role of chalcogen-bonding interactions in the binding of ebselen to the main protease  $\text{M}^{\text{Pro}}$  of SARS-CoV-2 has been demonstrated recently (Menendez *et al.*, 2020; Fellowes & White, 2022).



Given the strength of benzoselenazolone-based chalcogen-bond donors, we were interested in adapting the system to form other supramolecular architectures. We envisaged that the pyridin-3-yl-substituted benzoselenazolone 2-(pyridin-3-yl)-2,3-dihydro-1,2-benzoselenazol-3-one (**2**) might form an alternative one-dimensional chalcogen-bonded polymer, with the pyridine N atom fulfilling the role of chalcogen-bond acceptor. Pyridine-substituted ebselen derivative **2** was synthesized by reaction of the diselenide 2,2'-(diselane-1,2-diyl)dibenzoic acid (**3**) with excess thionyl chloride to give the electrophilic intermediate 2-(chloroselanyl)benzoyl chloride

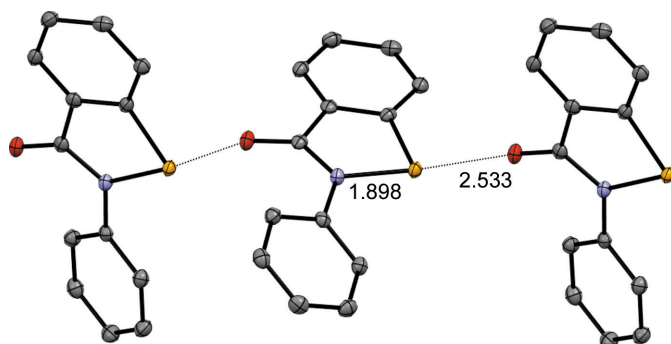


**Figure 1**  
The chalcogen-bonded chains in the crystal structure of ebselen **1**.

(**4**). The electrophile **4** was then treated with pyridin-3-amine (**5**) to assemble the benzoselenazolone ring (Scheme 1). Crystallization of the crude product from hot dimethylformamide (DMF) afforded light-brown plate-like single crystals of **2**.

## 2. Experimental

NMR spectra were recorded on a Varian 400 MHz spectrometer (see supporting information). Chemical shifts are reported in ppm relative to tetramethylsilane (TMS), referenced to the residual solvent signal. The integrals are in accordance with assignments and coupling constants are given in Hz. All reported  $^{13}\text{C}$  spectra are proton decoupled. Multiplicity is indicated as follows: *s* = singlet, *brs* = broad singlet, *d* = doublet, *m* = multiplet and *dd* = doublet of doublets.

### 2.1. Synthesis and crystallization

**2.1.1. Preparation of benzoselenazolone 2.** Diselenide **3** (1.2 g, 2.99 mmol) was refluxed in thionyl chloride (10 ml) for 30 min, after which the solid had dissolved. The excess thionyl chloride was removed by distillation and the residue triturated with dry hexane (20 ml). Removal of the hexane under reduced pressure gave the electrophilic reagent **4** as a pale-yellow solid which was used without further purification or characterization. The electrophilic reagent **4** was then added to a solution of pyridin-3-amine (**4**; 0.56 g, 2.99 mmol) in acetonitrile (10 ml) and anhydrous triethylamine (1 ml). The mixture was stirred at room temperature for 2 h, the solvent removed under reduced pressure and the residue crystallized from hot DMF giving compound **2** as off-white plates (m.p. 272–274 °C; yield 0.76 g, 90%).  $^1\text{H}$  NMR ( $d_6$ -DMSO):  $\delta$  8.85 (1H, *brs*), 8.43 (1H, *d*,  $J = 4.7$  Hz), 8.08 (1H, *d*,  $J = 8.1$  Hz), 8.04 (1H, *ddd*,  $J = 8.3, 7.2, 1.5$  Hz), 7.90 (1H, *dd*,  $J = 7.7, 1.4$  Hz), 7.68 (1H, *ddd*,  $J = 8.2, 2.7, 1.4$ ), 7.45–7.49 (1H, *m*).  $^{13}\text{C}$  NMR ( $d_6$ -DMSO):  $\delta$  166.16, 146.95, 145.97, 139.58, 137.27, 133.12, 132.44, 128.60, 128.45, 126.94, 126.55, 124.59.

**2.1.2. Preparation of 2-Me<sup>+</sup> iodide and 2-Me<sup>+</sup> tosylate.** Compound **2** (200 mg) in DMF (5 ml) was heated in the presence of excess methyl iodide (5 equiv.) or methyl tosylate (1.1 equiv.), respectively, giving quantitative conversion to 2-Me<sup>+</sup> iodide (m.p. 268–275 °C, decomposition) and 2-Me<sup>+</sup> tosylate (m.p. 212–214 °C).  $^1\text{H}$  NMR for 2-Me<sup>+</sup> iodide ( $d_6$ -DMSO):  $\delta$  9.47 (1H, *dd*,  $J = 1.8, 1.8$  Hz), 8.74 (1H, *d*,  $J = 5.9$  Hz), 8.71 (1H, *dd*,  $J = 7.6, 0.84$  Hz), 8.30 (1H, *d*,  $J = 8.3$ ), 8.11 (1H, *dd*,  $J = 7.7, 1.4$ ), 7.93 (1H, *dd*,  $J = 7.7, 1.4$  Hz), 7.7 (1H, *m*), 7.5 (1H, *ddd*,  $J = 8.0, 7.2, 1.0$  Hz), 4.37 (3H, *s*).  $^1\text{H}$  NMR for 2-Me<sup>+</sup> tosylate ( $d_6$ -DMSO):  $\delta$  9.52 (1H, *dd*,  $J = 1.9, 1.9$  Hz), 8.8 (1H, *d*,  $J = 5.9$  Hz), 8.77 (1H, *dd*,  $J = 8.4, 2.3$  Hz), 8.05–8.15 (3H, *m*), 7.93 (1H, *dd*,  $J = 7.8, 1.4$  Hz), 7.71 (1H, *ddd*,  $J = 8.3, 7.1, 1.5$  Hz), 7.51 (1H, *dd*,  $J = 7.5, 1.0$  Hz), 7.10 (2H, *d*,  $J = 7.8$  Hz), 4.38 (3H, *s*).

### 2.2. Refinement

Crystal data, data collection and structure refinement details are summarized in Table 1. The H atoms were located

**Table 1**  
Experimental details.

Experiments were carried out at 100 K using a Rigaku XtaLAB Synergy diffractometer with a Dualflex HyPix detector.

	<b>2</b>	<b>2-Me<sup>+</sup> iodide</b>	<b>2-Me<sup>+</sup> tosylate trihydrate</b>	<b>2-multipole</b>
Crystal data				
Chemical formula	C <sub>12</sub> H <sub>8</sub> N <sub>2</sub> OSe	C <sub>13</sub> H <sub>11</sub> N <sub>2</sub> OSe <sup>+</sup> ·I <sup>-</sup>	C <sub>13</sub> H <sub>11</sub> N <sub>2</sub> OSe <sup>+</sup> ·C <sub>7</sub> H <sub>7</sub> O <sub>3</sub> S <sup>-</sup> ·3H <sub>2</sub> O	C <sub>12</sub> H <sub>8</sub> N <sub>2</sub> OSe
<i>M<sub>r</sub></i>	275.16	417.10	515.43	275.16
Crystal system, space group	Monoclinic, <i>P</i> 2 <sub>1</sub> / <i>n</i>	Triclinic, <i>P</i> $\bar{1}$	Triclinic, <i>P</i> $\bar{1}$	Monoclinic, <i>P</i> 2 <sub>1</sub> / <i>n</i>
<i>a</i> , <i>b</i> , <i>c</i> (Å)	6.1087 (1), 14.2241 (2), 12.0630 (2)	7.0926 (1), 8.1329 (1), 11.8376 (1)	6.9412 (3), 12.1279 (4), 13.5994 (3)	6.1074 (1), 14.2227 (3), 12.0621 (2)
$\alpha$ , $\beta$ , $\gamma$ (°)	90, 103.594 (1), 90	84.618 (1), 82.243 (1), 77.756 (1)	70.426 (3), 83.774 (3), 83.585 (3)	90, 103.588 (2), 90
<i>V</i> (Å <sup>3</sup> )	1018.80 (3)	659.70 (1)	1068.83 (7)	1018.43 (3)
<i>Z</i>	4	2	2	4
Radiation type	Mo <i>K</i> $\alpha$	Mo <i>K</i> $\alpha$	Cu <i>K</i> $\alpha$	Mo <i>K</i> $\alpha$
$\mu$ (mm <sup>-1</sup> )	3.66	5.18	3.70	3.66
Crystal size (mm)	0.48 × 0.15 × 0.05	0.46 × 0.06 × 0.06	0.21 × 0.03 × 0.03	0.48 × 0.15 × 0.05
Data collection				
Absorption correction	Gaussian ( <i>CrysAlis PRO</i> ; Rigaku OD, 2020)	Gaussian ( <i>CrysAlis PRO</i> ; Rigaku OD, 2020)	Multi-scan ( <i>CrysAlis PRO</i> ; Rigaku OD, 2020)	Gaussian ( <i>CrysAlis PRO</i> ; Rigaku OD, 2020)
<i>T</i> <sub>min</sub> , <i>T</i> <sub>max</sub>	0.147, 1.000	0.351, 1.000	0.668, 1.000	0.147, 1.000
No. of measured, independent and observed reflections	98437, 14308, 9929 [ <i>I</i> > 2 $\sigma$ ( <i>I</i> )]	90106, 14487, 12038 [ <i>I</i> > 2 $\sigma$ ( <i>I</i> )]	15253, 4435, 3777 [ <i>I</i> > 2 $\sigma$ ( <i>I</i> )]	97589, 7174, 6298 [ <i>I</i> ≥ 2 $\sigma$ ( <i>I</i> )]
<i>R</i> <sub>int</sub> ( <i>sin</i> $\theta$ / $\lambda$ ) <sub>max</sub> (Å <sup>-1</sup> )	0.044 1.191	0.055 1.098	0.064 0.632	0.044 0.950
Refinement				
<i>R</i> [ <i>F</i> <sup>2</sup> > 2 $\sigma$ ( <i>F</i> <sup>2</sup> )], <i>wR</i> ( <i>F</i> <sup>2</sup> ), <i>S</i>	0.031, 0.072, 1.00	0.025, 0.058, 1.03	0.041, 0.104, 1.06	0.016, 0.023, 1.07
No. of reflections	14308	14487	4435	7174
No. of parameters	145	164	306	496
No. of restraints	0	0	6	22
H-atom treatment	H-atom parameters constrained	H-atom parameters constrained	H atoms treated by a mixture of independent and constrained refinement	All H-atom parameters refined
$\Delta\rho_{\max}$ , $\Delta\rho_{\min}$ (e Å <sup>-3</sup> )	1.25, -0.61	1.24, -1.68	0.89, -0.66	0.43, -0.41

Computer programs: *CrysAlis PRO* (Rigaku OD, 2020), *SHELXT* (Sheldrick, 2015a), *SHELXL2016* (Sheldrick, 2015b), *MoPro* (Jelsch *et al.*, 2005), *Mercury* (Macrae *et al.*, 2020) and *WinGX* (Farrugia, 2012).

in difference Fourier maps but were introduced in calculated positions and treated as riding on their parent atoms (C atoms). The H atoms of the water molecules were located in difference Fourier maps and refined isotropically.

Refinements for charge-density analysis of **2** were performed against *F*<sup>2</sup>, up to a maximum reciprocal resolution of

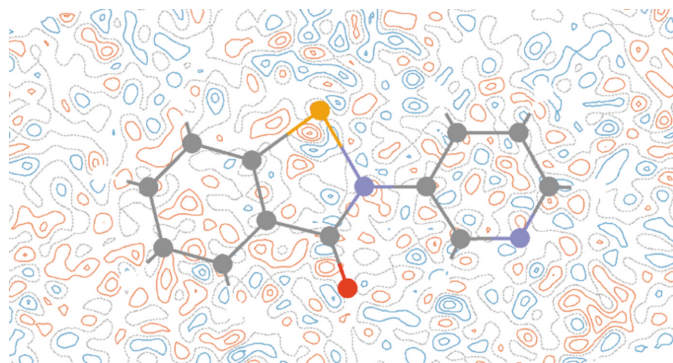


**Figure 2**  
Difference electron residuals from the multipole refinement of compound **2** with 0.05 e Å<sup>-3</sup> contours. Red contours are positive, blue are negative and dashed grey are zero.

0.95 Å<sup>-1</sup> for a total of 7174 independent reflections using the *MoPro* software (Guillot *et al.*, 2001). Beamstop-affected reflections were identified and excluded at the data reduction stage, and disagreeable frames were removed. The independent atom model (IAM) structure was first refined using *NoSpherA2* in *OLEX2* (Kleemiss *et al.*, 2021). This procedure generates aspherical scattering factors for the atoms in the crystal based on a density functional theory (DFT) calculation. The PBE0/def2TZVP level was used for this calculation, and *R1/wR2* values of 0.0281/0.0471 were obtained after convergence of the wavefunction calculation and crystallographic refinement. This model was used as a starting point for the multipole refinement in the *MoPro Suite* (Guillot *et al.*, 2001; Jelsch *et al.*, 2005). As the atomic anisotropic displacement parameters (ADPs) had been adequately determined by refinement using calculated scattering factors, charge density parameters were refined from the beginning, without an initial high-order refinement as is usual in charge density investigations. Statistical weights were used throughout the multipole refinement, and 2% of all reflections were marked as free. Multipole parameters were initialized from the ELMAM2 database for all atoms except for selenium, for which parameters were not available. The multipole expansion was

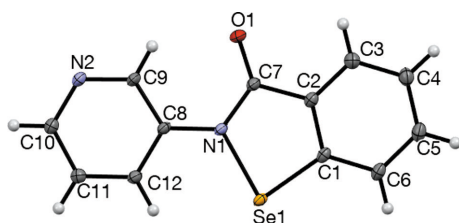


**Figure 3**  
The molecular structure of compound **2**, showing 50% probability displacement ellipsoids.

limited to a 32-pole level for the Se atom and to an octupole level for the other heavy atoms. H atoms were modelled at the quadrupole level. Default Slater-type functions were used for all atoms. Charge density symmetry constraints were applied, and kappas were constrained to be equal for chemically equivalent atoms. C–H bonds were constrained to neutron distances and idealized geometries, but  $U_{\text{iso}}$  values were refined freely. Initially, an overall scale factor was refined, and this was included in all subsequent refinements. Valence and multipole population parameters were then refined, followed by their respective kappas, and this cycle was repeated. When this had converged (shift/ $<0.001$ ),  $xyz$  and  $U^{ij}$  were refined. This procedure was repeated to convergence. All heavy atoms were then refined anharmonically (maximum order 3) until convergence, and the Gram–Charlier coefficients of each atom were compared with their estimated uncertainty. If no coefficient exceeded  $3\sigma$ , the atom was removed from the anharmonic refinement. Atoms Se1, O1, N2, C2, C3, C5, C7, C8, C9, C10, C11 and C12 displayed appreciable anharmonic motion, and were thus refined as such. An isotropic extinction parameter was introduced, which substantially reduced residual electron density around the Se atom. Kappa constraints were lifted gradually, followed by multipole symmetry constraints, then all parameters were refined together initially with heavy damping, which was reduced to zero in the final cycles. The final  $R1/wR2$  values were 0.016/0.023 and the goodness-of-fit (GoF) was 1.07.  $R_{\text{freec}}$  remained comparable to  $R1$  throughout the refinement, so we do not believe the model suffers from overfitting. The total number of refined parameters in the final cycle was 496, to give a data/parameter ratio of 14.4. The estimated average error in the electron density was  $0.0970 \text{ e } \text{\AA}^{-3}$ , with a maximum and minimum residual density of  $0.43/$

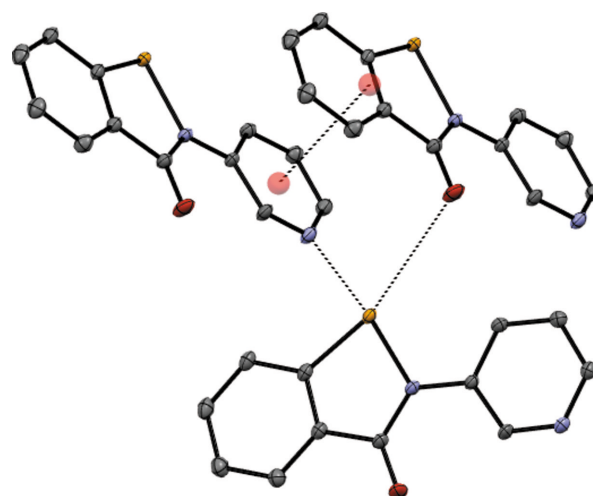


**Figure 5**  
The N...Se and O...Se chalcogen-bonding interactions and  $\pi$ – $\pi$  stacking interactions in the structure of compound **2**.

$-0.41 \text{ e } \text{\AA}^{-3}$ , which was randomly distributed through the asymmetric unit (Fig. 2).

### 3. Results and discussion

Pyridine-substituted benzoselenazolinone derivative **2** was synthesized by reaction of diselenide **3** (Scheme 1) with thionyl chloride giving the electrophilic selenium reagent **4** which was immediately coupled with pyridin-3-amine (**5**). Crystallization of the crude product from hot DMF afforded light-brown plate-like single crystals of **2** suitable for X-ray analysis. Heating compound **2** with methyl iodide or methyl tosylate in DMF gave **2-Me<sup>+</sup>** iodide and **2-Me<sup>+</sup>** tosylate, respectively. Crystals for all samples were obtained from DMF.

#### 3.1. Structure analysis for **2**

The displacement ellipsoid plot for **2** is presented in Fig. 3, while selected geometrical parameters are given in Table 2. The molecular structure is essentially planar, with an r.m.s. deviation of  $0.0357 \text{ \AA}$  for the non-H atoms. The conformation about the N1–C8 bond sees the pyridine N atom (N2) on the opposite side to the Se atom (Se1); this conformation may be

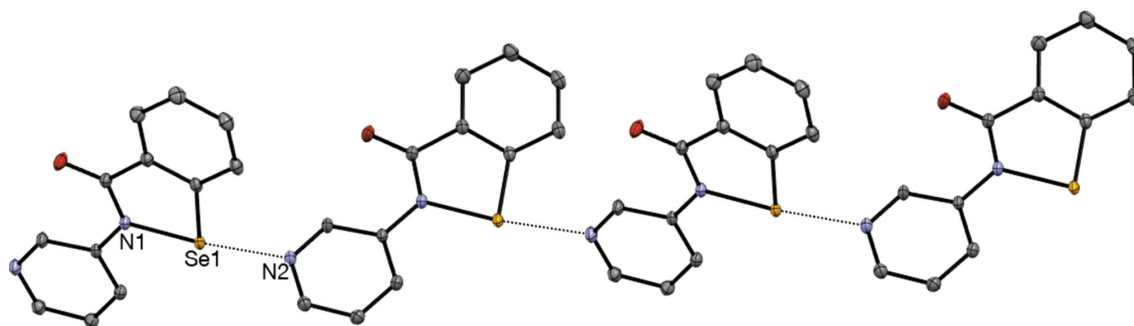


**Figure 4**  
The chalcogen-bonded chains of compound **2** propagating along the  $ac$  diagonal.



preferred due to a favourable electrostatic contact between the polarized H atom attached to C9 and amide atom O1, or alternatively this conformation is a consequence of the crystal packing (as discussed below), or both. The structure is characterized by the presence of a strong intermolecular chalcogen-bonding interaction involving the polarized Se1–N1 bond [ $\text{N2}^i \cdots \text{Se1} = 2.3831(6) \text{ \AA}$  and  $\text{N2}^i \cdots \text{Se1} - \text{N1} = 177.44(2)^\circ$ ; symmetry code: (i)  $x - \frac{1}{2}, -y + \frac{1}{2}, z + \frac{1}{2}$ ] which propagates along the *ac* diagonal (Fig. 4). This strong chalcogen bond combines with a weaker intermolecular chalcogen-bonding interaction involving the less polarized Se1–C1 bond with the amide carbonyl O atom [ $\text{O1}^{ii} \cdots \text{Se1} = 3.3347(7) \text{ \AA}$  and  $\text{O1}^{ii} \cdots \text{Se1} - \text{C1} = 165.77(2)^\circ$ ; symmetry code: (ii)  $x + \frac{1}{2}, -y + \frac{1}{2}, z + \frac{1}{2}$ ], and a  $\pi$ -stacking interaction between the pyridine ring [related by the symmetry code  $(x - \frac{1}{2}, -y + \frac{1}{2}, z + \frac{1}{2})$ ] and the benzoselenazolinone ring system [related by the symmetry code  $(x + \frac{1}{2}, -y + \frac{1}{2}, z + \frac{1}{2})$ ], having a centroid–centroid distance of 3.412 Å (Fig. 5). These three intermolecular interactions, while not mutually orthogonal, do result in a three-dimensional supramolecular network (Fig. 6). It is worth making a comparison of the structure of **2**, which contains  $\text{N} \cdots \text{Se1}(-\text{N1})$  chains in the crystal, with the parent ebsele (**1**) (Thomas *et al.*, 2015), which is characterized by  $\text{C}=\text{O} \cdots \text{Se1} - \text{N1}$  chalcogen-bonded chains. The  $\text{C}=\text{O} \cdots \text{Se1}$  interaction in **1** is characterized by an  $\text{Se} \cdots \text{O}$  distance of 2.533 (1) Å (polymorph 2), which represents a contraction of 0.87 Å compared to the van der Waals radii for Se and O. In comparison, the  $\text{N2} \cdots \text{Se1}(-\text{N1})$  distance of 2.3831 (6) Å in **2** is contracted by 1.06 Å from the sum of the van der Waals radii for Se and N of 3.45 Å (Bondi, 1964), suggesting that the  $\text{N} \cdots \text{Se}(-\text{N})$  chalcogen-bonding interaction in **2** is significantly stronger than the  $\text{O} \cdots \text{Se}(-\text{N})$  interaction in **1**. This result is consistent with the pyridine N atom in **2** being a significantly stronger chalcogen-bond acceptor than the amide O atom in **1** and agrees with previous results from cocrystal derivatives of **1** (Fellowes *et al.*, 2019). In addition to dispersion forces, the chalcogen bond has both an electrostatic component (attraction between the positively

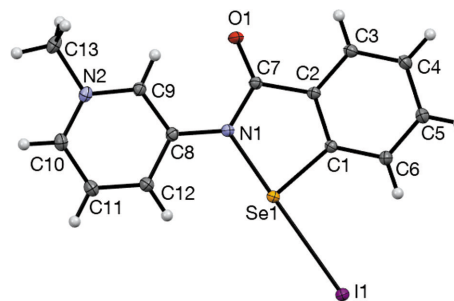


**Figure 7**  
The molecular structure of **2-Me**<sup>+</sup> iodide, showing 50% probability displacement ellipsoids.

charged  $\sigma$ -hole on the selenium and the electron-rich chalcogen-bond acceptor) and an orbital interaction component [in which the electron-rich chalcogen-bond acceptor (highest occupied molecular orbital, HOMO) donates electron density into the low-lying Se–N  $\sigma^*$  antibonding orbital (lowest unoccupied molecular orbital, LUMO) on the Se atom] (Pascoe *et al.*, 2017; Kolář & Hobza, 2016); this latter interaction results in weakening and lengthening of the internal Se1–N bond distance. Consistent with the apparently stronger  $\text{N} \cdots \text{Se}$  interaction in **2** versus the  $\text{O} \cdots \text{Se}$  interaction in **1** is the significant lengthening of the Se1–N1 distance [1.9788 (5) Å] for **2** compared to that [1.905 (1) Å] for **1**, suggesting a significantly increased population of the Se–N  $\sigma^*$  antibonding orbital in **2**.

### 3.2. Structure analysis for 2-Me<sup>+</sup> iodide

The displacement ellipsoid plot for **2-Me**<sup>+</sup> iodide is presented in Fig. 7. The structure is essentially planar, with an r.m.s. deviation of 0.038 Å for the non-H atoms of the cation. The iodide counter-ion, which is strongly associated with the cation, lies close to this plane [deviation 0.131 (1) Å]. The nature of the interaction of the iodide anion with the cation is by an  $\text{I}^- \cdots \text{Se}$  chalcogen-bonding interaction [ $\text{I1} \cdots \text{Se1} =$

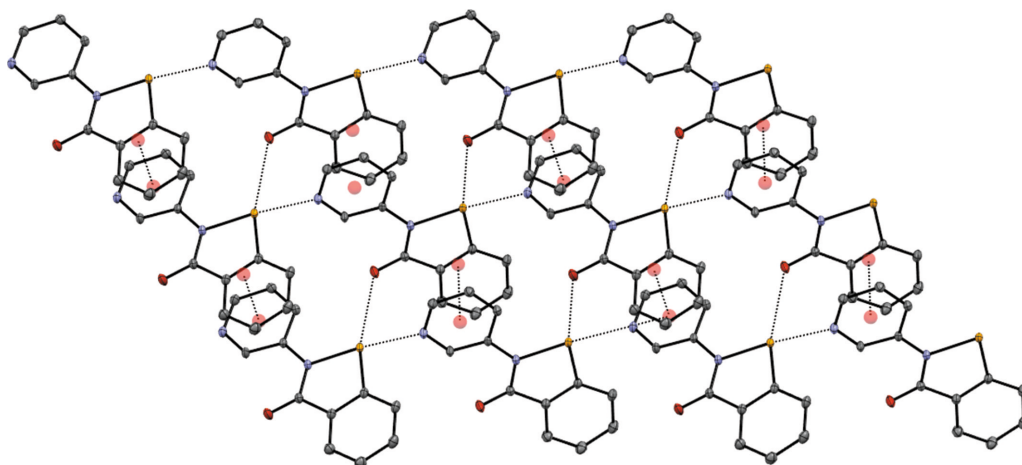


**Figure 6**  
Partial packing diagram of compound **2**, showing the three-dimensional network built up of chalcogen-bonding interactions and  $\pi$ - $\pi$  stacking interactions, viewed parallel to the (010) plane.

**Table 2**

 Selected geometric parameters (Å, °) for **2**.

C1—C2	1.3927 (9)	C8—C9	1.4073 (8)
C1—Se1	1.9037 (6)	C9—N2	1.3388 (8)
C2—C7	1.4715 (8)	C10—N2	1.3354 (9)
C7—O1	1.2349 (8)	N1—Se1	1.9788 (5)
C7—N1	1.3653 (8)	Se1—N2 <sup>i</sup>	2.3831 (6)
C8—N1	1.4007 (7)		
C2—C1—Se1	112.57 (4)	C7—N1—Se1	115.23 (4)
C6—C1—Se1	128.04 (5)	C8—N1—Se1	120.27 (4)
C1—C2—C7	117.65 (5)	C10—N2—C9	120.38 (5)
N1—C7—C2	110.55 (5)	C1—Se1—N2 <sup>i</sup>	90.65 (2)
C7—N1—C8	124.50 (5)	N1—Se1—N2 <sup>i</sup>	174.44 (2)

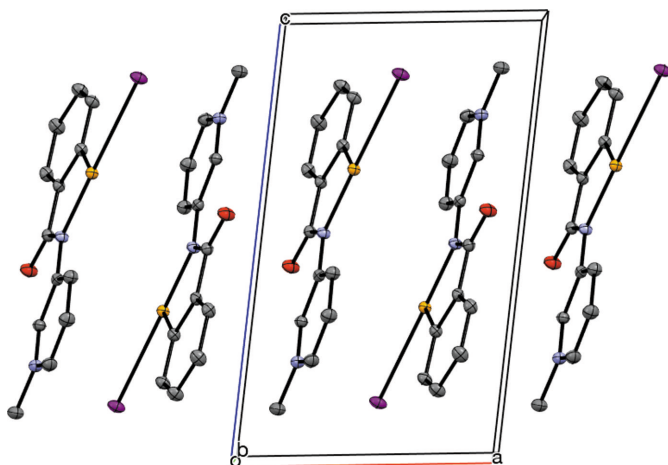
 Symmetry code: (i)  $x - \frac{1}{2}, -y + \frac{1}{2}, z + \frac{1}{2}$ .

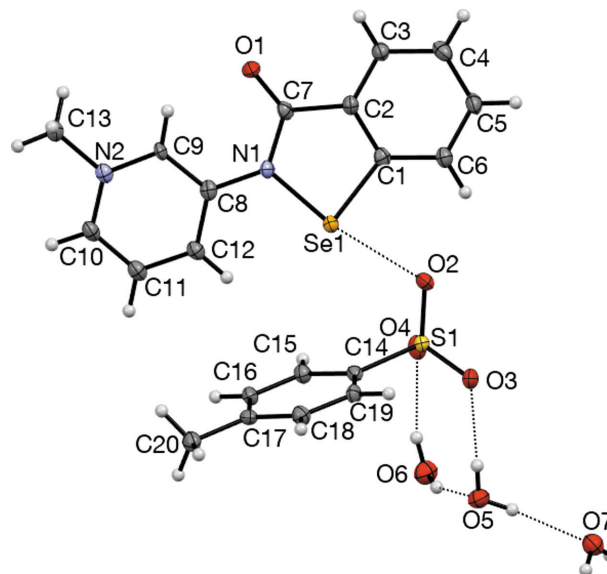
**Table 3**

 Selected geometric parameters (Å, °) for **2-Me<sup>+</sup>** iodide.

C1—C2	1.3968 (10)	C8—C9	1.4006 (10)
C1—Se1	1.9108 (7)	C9—N2	1.3514 (10)
C2—C7	1.4695 (11)	C10—N2	1.3430 (12)
C7—O1	1.2339 (9)	C13—N2	1.4784 (11)
C7—N1	1.3762 (10)	N1—Se1	2.0053 (6)
C8—N1	1.3907 (10)	Se1—I1	2.9882 (1)
C2—C1—Se1	113.17 (5)	C8—N1—Se1	120.73 (5)
C6—C1—Se1	126.93 (6)	C10—N2—C9	122.78 (7)
C1—C2—C7	117.81 (6)	C10—N2—C13	120.40 (7)
N1—C7—C2	110.63 (6)	C9—N2—C13	116.82 (7)
C7—N1—C8	124.27 (6)	C1—Se1—I1	95.85 (2)
C7—N1—Se1	114.94 (5)	N1—Se1—I1	178.85 (2)

2.9882 (1) Å and I1...Se1—N1 = 178.85 (2)°], which is perfectly aligned with the antipode of the polarized Se1—N1 bond, is well within the sum of the van der Waals radii for I and Se (3.88 Å) and is approaching the bond distance for a formal Se—I covalent bond; the Se—I distance in mesityl selenium iodide is 2.536 (1) Å (Jeske *et al.*, 2002) and in 2,4,6-tri-*tert*-butylphenylselenium iodide is 2.529 Å (du Mont *et al.*, 1987). The strength of this chalcogen bond is not only apparent from the short I<sup>−</sup>...Se contact, but also from the significant lengthening of the internal Se—N1 bond distance, which is 2.0053 (6) Å compared to 1.905 Å in the parent


**Figure 8**

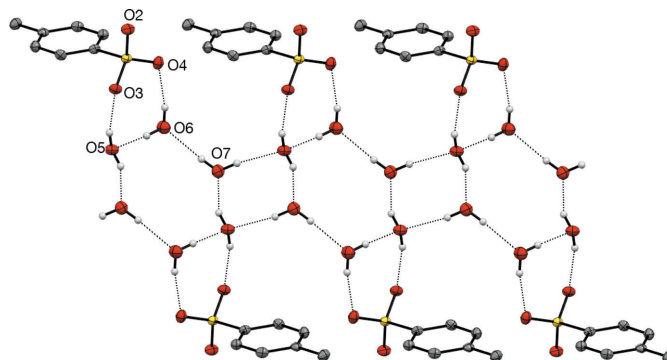
 The  $\pi$ - $\pi$  stacking interactions in the structure of **2-Me<sup>+</sup>** iodide.

**Figure 9**

 The molecular structure of **2-Me<sup>+</sup>** tosylate trihydrate, showing 50% probability displacement ellipsoids.

molecule **1**. Perhaps the I<sup>−</sup>...Se1—N1 moiety is best described as a 3-centre-4-electron bond. The crystal packing of **2-Me<sup>+</sup>** iodide is dominated by strong  $\pi$ - $\pi$  stacking interactions along the *a* axis between molecules of the complex, with each planar molecule sandwiched between two parallel molecules related by the symmetry codes ( $-x + 1, -y + 1, -z + 1$ ), with an interplanar spacing of 3.4146 (8) Å, and ( $-x + 2, -y + 1, -z + 1$ ), with an interplanar spacing of 3.295 (1) Å (Fig. 8). Selected geometrical parameters are given in Table 3.

### 3.3. Structure analysis for **2-Me<sup>+</sup>** tosylate

The **2-Me<sup>+</sup>** tosylate derivative, represented by the displacement ellipsoid plot in Fig. 9, crystallizes as a trihydrate, which presumably forms as it satisfies the coordination requirements of the tosylate anion, with its three O atoms participating in a number of interactions, including a chal-


**Figure 10**

 The hydrogen-bonding interactions in the structure of **2-Me<sup>+</sup>** tosylate trihydrate. The undulating chain extends along the *a* axis.

**Table 4**Selected geometric parameters (Å, °) for **2-Me**<sup>+</sup> tosylate trihydrate.

C1—C2	1.398 (4)	C10—N2	1.350 (4)
C1—Se1	1.901 (3)	C13—N2	1.494 (4)
C2—C7	1.471 (4)	C14—S1	1.767 (3)
C7—O1	1.221 (4)	N1—Se1	1.926 (2)
C7—N1	1.388 (4)	O2—S1	1.466 (2)
C8—N1	1.395 (4)	O3—S1	1.459 (2)
C8—C9	1.404 (4)	O4—S1	1.454 (2)
C9—N2	1.352 (4)	O2—Se1	2.553 (2)
C6—C1—Se1	126.9 (2)	C8—N1—Se1	119.21 (19)
C2—C1—Se1	112.0 (2)	C10—N2—C9	123.4 (3)
C1—C2—C7	116.9 (3)	C10—N2—C13	119.0 (3)
N1—C7—C2	110.7 (2)	C9—N2—C13	117.6 (2)
C7—N1—C8	125.7 (2)	C1—Se1—N1	85.33 (12)
C7—N1—Se1	115.07 (19)	O2—Se1—N1	170.57 (10)

cogen-bonding interaction with the Se atom, in addition to a number of hydrogen-bonding interactions involving the three water molecules. The water molecules form an undulating hydrogen-bonded tape parallel to the *a* axis, consisting of alternating six-membered rings fused to four-membered rings, referred to as the T4(2)6(2) motif (Golz & Strohmman, 2015; Custelcean *et al.*, 2000). Each six-membered ring provides four hydrogen bonds to two tosylate anions related by inversion (Fig. 10). The remaining tosylate O atom (O2) forms a chalcogen bond to the Se atom of the cation [O2...Se1 = 2.553 (2) Å and O2...Se—N1 = 170.57 (10)°]; the planar cations are approximately orthogonal to the propagating direction of the water tape and allows for interdigitation from a neighbouring tape by  $\pi$ - $\pi$  stacking of the benzisoselenazolinone moieties. Each cation is sandwiched between two parallel cations, with interplanar spacings of 3.383 (7) [at  $(-x + 2, -y + 1, -z + 1)$ ] and 3.405 (7) Å [at  $(-x + 1, -y + 1, -z + 1)$ ] (Fig. 11), resulting in a two-dimensional network parallel to the (011) plane. Despite the chalcogen-bond interaction in **2-Me**<sup>+</sup> tosylate involving a negatively charged tosylate O atom (quenched to a certain extent by the numerous hydrogen-bonding interactions), the O2...Se1 distance of 2.553 (2) Å (a contraction of 0.857 Å from the sum of the van der Waals radii of 3.41 Å) is clearly weaker than that in the neutral derivative involving the pyridine N atom [N2<sup>i</sup>...Se1 = 2.3831 (6) Å, a contraction of 1.006 Å from the sum of the van der Waals radii for N and Si of 3.45 Å]. Selected geometrical and hydrogen-bond parameters are given in Tables 4 and 5, respectively. Consistent with this is the

**Table 5**Hydrogen-bond geometry (Å, °) for **2-Me**<sup>+</sup> tosylate trihydrate.

<i>D</i> —H... <i>A</i>	<i>D</i> —H	H... <i>A</i>	<i>D</i> ... <i>A</i>	<i>D</i> —H... <i>A</i>
C9—H9...O1	0.93	2.09	2.734 (4)	125
O5—H5A...O3	0.82 (1)	1.99 (1)	2.786 (3)	166 (4)
O5—H5A...S1	0.82 (1)	3.01 (2)	3.698 (2)	144 (3)
O5—H5B...O7	0.82 (1)	1.99 (4)	2.758 (3)	155 (8)
O6—H6A...O4	0.82 (1)	2.27 (2)	3.045 (3)	159 (5)
O6—H6B...O5	0.82 (1)	1.99 (2)	2.782 (4)	162 (7)
O7—H7A...O6 <sup>i</sup>	0.82 (1)	1.97 (1)	2.783 (4)	176 (5)
O7—H7B...O5 <sup>ii</sup>	0.82 (1)	1.97 (1)	2.786 (4)	172 (6)

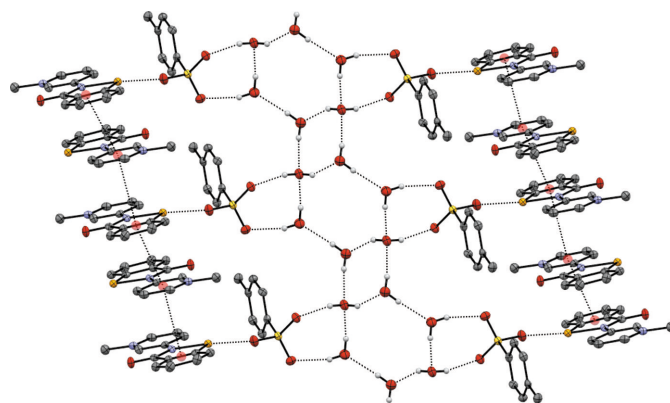
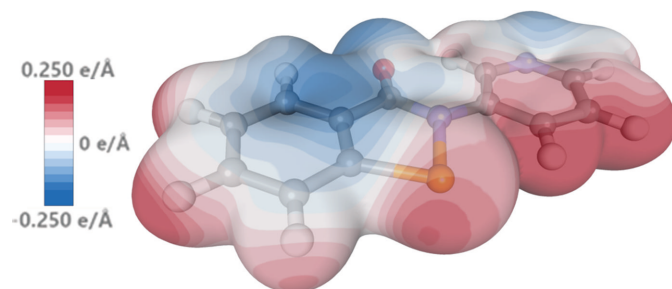
Symmetry codes: (i)  $-x + 2, -y + 2, -z + 2$ ; (ii)  $-x + 1, -y + 2, -z + 2$ .**Table 6**Selected geometric parameters (Å, °) for **2**-multipole.

Se1—N1	1.9799 (5)	N2—C10	1.334 (3)
Se1—C1	1.9025 (6)	N2—C9	1.341 (2)
O1—C7	1.243 (2)	C1—C2	1.3914 (18)
N1—C7	1.363 (2)	C2—C7	1.467 (2)
N1—C8	1.3982 (17)	C8—C9	1.412 (2)
N1—Se1—C1	84.01 (2)	C10—N2—C9	120.50 (18)
Se1—N1—C7	115.04 (9)	Se1—C1—C2	112.38 (8)
Se1—N1—C8	120.13 (7)	Se1—C1—C6	128.12 (4)
C7—N1—C8	124.83 (11)	N1—C7—C2	110.68 (13)

internal Se—N1 bond of 1.926 (2) Å in **2-Me**<sup>+</sup> tosylate (Table 6), which while significantly lengthened compared to the parent ebsele (1.905 Å), is much less so than in **2** [Se1—N1 = 1.9788 (5) Å], reflecting the greater extent of the  $n_{\text{N}}-\sigma^*_{\text{Se-N}}$  orbital interaction compared to the  $n_{\text{O}}-\sigma^*_{\text{Se-N}}$  interaction.

### 3.4. Charge density analysis for **2**

We used the experimental electron density from the multipole model to explore the electronic features of the chalcogen bond in **2**. Firstly, the electrostatic potential was mapped onto the 0.05 a.u. electron-density isosurface, which revealed a strongly electropositive region along the extension of the Se—N bond, *i.e.* the hole. Also visible were the lone

**Figure 11**Hydrogen bonding, chalcogen bonding and  $\pi$ - $\pi$  stacking in the structure of **2-Me**<sup>+</sup> tosylate trihydrate.**Figure 12**Experimentally determined electrostatic potential for compound **2** mapped onto the 0.05 a.u. isosurface.

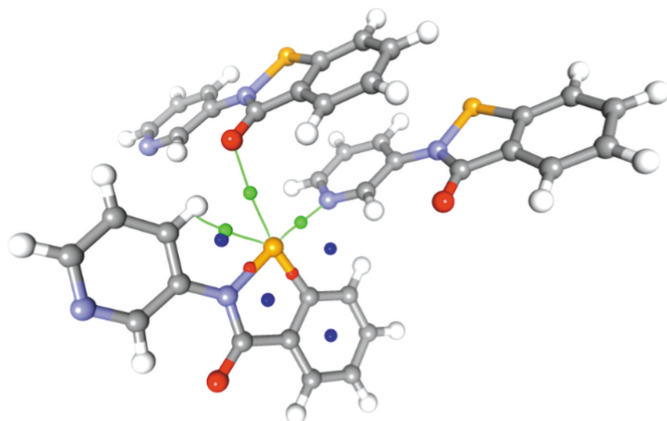


**Figure 13**  
Critical points (CPs) in the vicinity of the Se atom for compound **2**. (3,−1) CPs are shown in red (intramolecular) and green (intermolecular), and (3,+1) CPs are shown in blue.

pairs of the O and pyridyl N atom, and electron density above and below the  $\pi$ -system (Fig. 12).

The topology of the electron density was also analysed within the QTAIM framework (Bader, 1991), and bond paths corresponding to the Se $\cdots$ N and Se $\cdots$ O chalcogen bonds were found, along with associated bond critical points (BCPs; Fig. 13). The electron density at the BCP for the shorter Se $\cdots$ N chalcogen bond of  $0.340 \text{ e } \text{\AA}^{-3}$  is significantly larger than that for the Se $\cdots$ O chalcogen bond of  $0.042 \text{ e } \text{\AA}^{-3}$ . The topological parameters associated with these CPs are given in Table 7. The electron density and Laplacian at the critical point ( $\rho_{\text{CP}}$  and  $\nabla^2 \rho_{\text{CP}}$  for CP<sub>Se1–N2</sub>) are consistent with a closed-shell interaction, but we were intrigued by a number of observations which indicate that this may not be the case. Firstly, the endocyclic Se1–N1 bond is lengthened appreci-

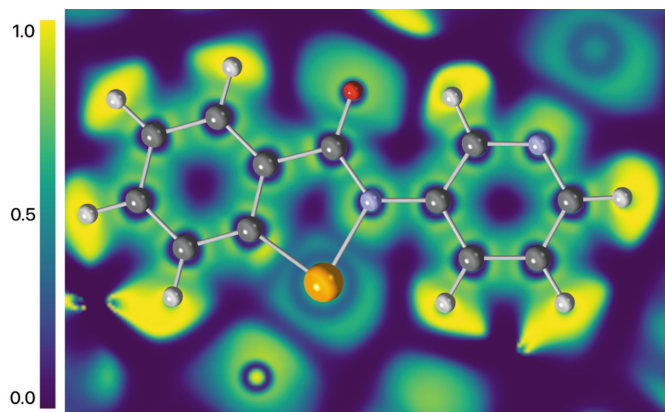


**Figure 14**  
Electron localization function (ELF) in the plane of the ring system for compound **2**.

ably compared to a gas-phase optimized structure [1.9801 (4) *versus* 1.8585 Å; Fellowes & White, 2022], suggestive of an  $n_{\text{N}}-\sigma^*$  delocalization, leading to partial occupation of the antibonding orbital and thus a lengthening of this bond. Secondly, this same bond has similar topological parameters at the CP to those of the chalcogen bond, which may indicate that the Se atom is participating in a 3-centre–4-electron bond between the two N atoms. Notably, the electronic energy density at the critical point  $H_{\text{CP}} = G_{\text{CP}} + V_{\text{CP}}$  is less than zero, corresponding to a dominant potential energy term ( $V_{\text{CP}}$ ), which is strongly indicative of electron sharing (Cremer & Kraka, 1984; Bone & Bader, 1996). This can be contrasted with the much weaker Se1–O1 chalcogen bond, where the kinetic energy ( $G_{\text{CP}}$ ) dominates.

The electron localization function (ELF) (Becke & Edgecombe, 1990) is a measure of the probability of finding an

**Table 7**  
Topological parameters at bond critical points (CPs) in the vicinity of the Se atom for **2**.

Critical point	Distance (Å)	$\rho_{\text{CP}}$ ( $\text{e } \text{\AA}^{-3}$ )	$\nabla^2 \rho_{\text{CP}}$ ( $\text{e } \text{\AA}^{-5}$ )	$G_{\text{CP}}$ ( $\text{kJ mol}^{-1} \text{ Bohr}^{-3}$ )	$V_{\text{CP}}$ ( $\text{kJ mol}^{-1} \text{ Bohr}^{-3}$ )	ELF
Se1–N2	2.3807 (9)	0.3402	2.9100	104.7	−130.15	0.196
Se1–O1	3.3328 (7)	0.0420	0.5077	10.81	−7.79	0.022
Se1–N1	1.9801 (4)	0.7782	5.3660	303.37	−460.6	0.351
Se1–C1	1.9028 (3)	0.9873	4.3030	384.34	−651.48	0.374

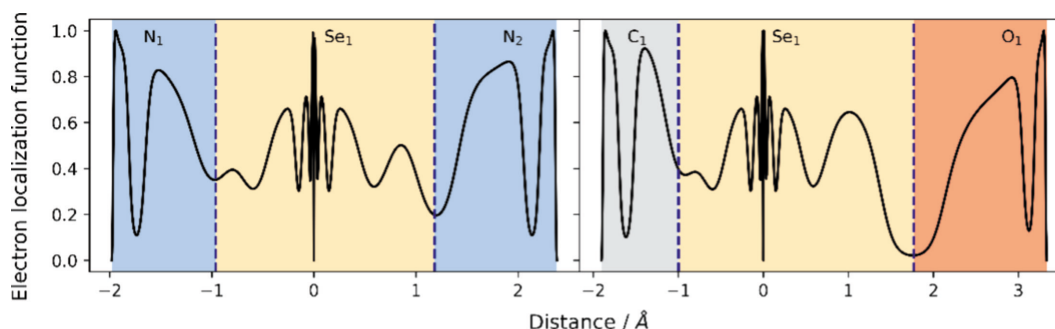


**Figure 15**  
ELF plotted along the N1–Se1–N2 and C1–Se1–O1 bonds for compound **2**. BCPs are shown as vertical dashed lines.



electron of like spin in the vicinity of a fictitious reference electron. It recovers the orbital structure of atoms, while not requiring any knowledge of a wavefunction. An ELF of 1 corresponds to complete localization of an electron pair, a value of  $\frac{1}{2}$  corresponds to a uniform electron gas-like delocalization, while a value of 0 denotes the border between electron pairs. The ELF in the plane of the aromatic system is plotted in Fig. 14, which shows partial electron localization in the Se1–N1 chalcogen bond, lending further support to the hypothesis that this is not a closed-shell interaction. The ELF along both the strong N1–Se1–N2 chalcogen bond and the weak C1–Se1–O1 chalcogen bond is plotted in Fig. 15, clearly showing the difference in ELF at the BCP of these two contrasting cases. In the stronger chalcogen bond, the ELF is approximately 0.2, while in the weak chalcogen bond it is almost zero.

#### 4. Conclusions

The crystal structure of the pyridine-substituted benzisosele-nazolinone **2** is dominated by strong intermolecular N $\cdots$ Se(–N) chalcogen bonding, where the N $\cdots$ Se distance of 2.3831 (6) Å is well within the sum of the van der Waals radii for N and Se (3.34 Å). This strong interaction results in significant lengthening of the internal N–Se distance, consistent with a significant orbital interaction component to the N $\cdots$ Se chalcogen bond. Much weaker intermolecular O $\cdots$ Se chalcogen bonding occurs between the amide-like O atom in **2** and the less polarized C–Se bond in this structure. Charge density analysis of **2** using multipole refinement of high-resolution data revealed the presence of a positive electrostatic surface potential at the antipode to the Se–N1 bond corresponding to the  $\sigma$ -hole. Topological analysis of the electron-density distribution in **2** within the QTAIM framework revealed bond paths and (3,–1) BCPs for the N $\cdots$ Se–N moiety consistent with a closed-shell interaction. However, the potential energy term suggests a significant contribution from electron sharing. Analysis of the electron localization function (ELF) for the strong N $\cdots$ Se and the weak O $\cdots$ Se chalcogen-bonding interactions in the structure of **2** suggests significant electron sharing in the former interaction and a largely electrostatic interaction in the latter. Conversion of **2** to its N-methylated derivatives by reaction with methyl iodide and methyl tosylate removes the possibility of N $\cdots$ Se intermolecular chalcogen bonding and instead structures are obtained where the iodide and tosylate counter-ions fulfill the role of chalcogen-bond acceptor, with a strong I $\cdots$ Se interaction in the iodide salt and a weaker *p*-Tol-SO $_3^-$  $\cdots$ Se interaction in the tosylate salt.

#### Acknowledgements

We thank the Australian Research Council for the award of an RTF scholarship (TF). Open access publishing facilitated by The University of Melbourne, as part of the Wiley – The University of Melbourne agreement via the Council of Australian University Librarians.

#### References

- Bader, R. (1991). *Chem. Rev.* **91**, 893–928.  
 Becke, A. D. & Edgecombe, K. E. (1990). *J. Chem. Phys.* **92**, 5397–5403.  
 Bondi, A. (1964). *J. Phys. Chem.* **68**, 441–451.  
 Bone, R. G. A. & Bader, R. F. W. (1996). *J. Phys. Chem.* **100**, 10892–10911.  
 Cremer, D. & Kraka, E. (1984). *Croat. Chem. Acta*, **57**, 1259–1281.  
 Custelcean, R., Afloaraei, C., Vlassa, M. & Polverejan, M. (2000). *Angew. Chem. Int. Ed.* **39**, 3094–3096.  
 Eckstein, B. J., Brown, L. C., Noll, B. C., Moghadassnia, M. P., Balaich, G. J. & McGuirk, C. M. (2021). *J. Am. Chem. Soc.* **143**, 20207–20215.  
 Farrugia, L. J. (2012). *J. Appl. Chem.* **45**, 849–854.  
 Fellowes, T., Skene, C. E., Martin, R. F., Lobachevsky, P., Owyong, T. C., Hong, Y. & White, J. M. (2022). *Arkivoc*, pp. S1–S14.  
 Fellowes, T., Van Koevorden, M. P. & White, J. M. (2020). *CrystEngComm*, **22**, 4023–4029.  
 Fellowes, T. & White, J. M. (2019). *CrystEngComm*, **21**, 1539–1542.  
 Fellowes, T. & White, J. M. (2022). *J. Mol. Model.* **28**, 66.  
 Golz, C. & Strohmman, C. (2015). *Acta Cryst.* **E71**, 564–566.  
 Guillot, B., Viry, L., Guillot, R., Lecomte, C. & Jelsch, C. (2001). *J. Appl. Cryst.* **34**, 214–223.  
 Jelsch, C., Guillot, B., Lagoutte, A. & Lecomte, C. (2005). *J. Appl. Cryst.* **38**, 38–54.  
 Jeske, J., Jones, P. G., von Salzen, A. M. & Mont, W.-W. (2002). *Acta Cryst.* **E58**, o350–o352.  
 Kleemiss, F., Dolomanov, O. V., Bodensteiner, M., Peyermhoff, N., Midgley, L., Bourhis, L. J., Genoni, A., Malaspina, L. A., Jayatilaka, D., Spencer, J. L., White, F., Grundkötter-Stock, B., Steinhauer, S., Lentz, D., Puschmann, H. & Grabowsky, S. (2021). *Chem. Sci.* **12**, 1675–1692.  
 Kolář, M. H. & Hobza, P. (2016). *Chem. Rev.* **116**, 5155–5187.  
 Macrae, C. F., Sovago, I., Cottrell, S. J., Galek, P. T. A., McCabe, P., Pidcock, E., Platings, M., Shields, G. P., Stevens, J. S., Towler, M. & Wood, P. A. (2020). *J. Appl. Cryst.* **53**, 226–235.  
 Menendez, C. A., Bylehn, F., De Perez-Lemus, G. R., Alvarado, W. & Pablo, J. J. (2020). *Sci. Adv.* **6**, eabd3045.  
 Mont, W. du, Kubiniok, S., Peters, K. & von Schnering, H. (1987). *Angew. Chem. Int. Ed. Engl.* **26**, 780–781.  
 Pascoe, D. J., Ling, K. B. & Cockroft, S. L. (2017). *J. Am. Chem. Soc.* **139**, 15160–15167.  
 Rigaku OD (2020). *CrysAlis PRO*. Rigaku Oxford Diffraction Ltd, Yarnton, Oxfordshire, England.  
 Sheldrick, G. M. (2015a). *Acta Cryst.* **A71**, 3–8.  
 Sheldrick, G. M. (2015b). *Acta Cryst.* **C71**, 3–8.  
 Thomas, S. P., Satheeshkumar, K., Mughesh, G. & Guru Row, T. (2015). *Chem. Eur. J.* **21**, 6793–6800.

## supporting information

*Acta Cryst.* (2023). C79, 43-51 [https://doi.org/10.1107/S2053229623000062]

## High-resolution structural study on pyridin-3-yl ebselen and its *N*-methylated tosylate and iodide derivatives

**Ruyi Xu, Thomas Fellowes and Jonathan M. White**

### Computing details

For all structures, data collection: *CrysAlis PRO* (Rigaku OD, 2020); cell refinement: *CrysAlis PRO* (Rigaku OD, 2020); data reduction: *CrysAlis PRO* (Rigaku OD, 2020); program(s) used to solve structure: SHELXT (Sheldrick, 2015a). Program(s) used to refine structure: *SHELXL2016* (Sheldrick, 2015b) for (2), 2-MeIodide, 2-Metosylate; MoPro (Jelsch *et al.*, 2005) for 2-multipole. For all structures, molecular graphics: *Mercury* (Macrae *et al.*, 2020); software used to prepare material for publication: *WinGX* (Farrugia, 2012).

### 2-(Pyridin-3-yl)-2,3-dihydro-1,2-benzoselenazol-3-one (2)

#### Crystal data

C<sub>12</sub>H<sub>8</sub>N<sub>2</sub>OSe

$M_r = 275.16$

Monoclinic, *P*2<sub>1</sub>/*n*

$a = 6.1087$  (1) Å

$b = 14.2241$  (2) Å

$c = 12.0630$  (2) Å

$\beta = 103.594$  (1)°

$V = 1018.80$  (3) Å<sup>3</sup>

$Z = 4$

$F(000) = 544$

$D_x = 1.794$  Mg m<sup>-3</sup>

Mo  $K\alpha$  radiation,  $\lambda = 0.71073$  Å

Cell parameters from 30338 reflections

$\theta = 3.3\text{--}56.9^\circ$

$\mu = 3.66$  mm<sup>-1</sup>

$T = 100$  K

Plate, colourless

$0.48 \times 0.15 \times 0.05$  mm

#### Data collection

Rigaku XtaLAB Synergy  
diffractometer with a Dualflex HyPix detector

Radiation source: micro-focus sealed X-ray  
tube, PhotonJet (Mo) X-ray Source

Mirror monochromator

$\omega$  scans

Absorption correction: gaussian  
(*CrysAlis PRO*; Rigaku OD, 2020)

$T_{\min} = 0.147$ ,  $T_{\max} = 1.000$

98437 measured reflections

14308 independent reflections

9929 reflections with  $I > 2\sigma(I)$

$R_{\text{int}} = 0.044$

$\theta_{\max} = 57.9^\circ$ ,  $\theta_{\min} = 2.9^\circ$

$h = -8 \rightarrow 14$

$k = -33 \rightarrow 33$

$l = -28 \rightarrow 28$

#### Refinement

Refinement on  $F^2$

Least-squares matrix: full

$R[F^2 > 2\sigma(F^2)] = 0.031$

$wR(F^2) = 0.072$

$S = 1.00$

14308 reflections

145 parameters

0 restraints

Hydrogen site location: inferred from  
neighbouring sites

H-atom parameters constrained

$$w = 1/[\sigma^2(F_o^2) + (0.0317P)^2 + 0.1363P]$$

where  $P = (F_o^2 + 2F_c^2)/3$   
 $(\Delta/\sigma)_{\max} = 0.003$

$$\Delta\rho_{\max} = 1.25 \text{ e } \text{\AA}^{-3}$$

$$\Delta\rho_{\min} = -0.61 \text{ e } \text{\AA}^{-3}$$

*Special details*

**Geometry.** All esds (except the esd in the dihedral angle between two l.s. planes) are estimated using the full covariance matrix. The cell esds are taken into account individually in the estimation of esds in distances, angles and torsion angles; correlations between esds in cell parameters are only used when they are defined by crystal symmetry. An approximate (isotropic) treatment of cell esds is used for estimating esds involving l.s. planes.

*Fractional atomic coordinates and isotropic or equivalent isotropic displacement parameters ( $\text{\AA}^2$ )*

	x	y	z	$U_{\text{iso}}^*/U_{\text{eq}}$
C1	0.26249 (10)	0.37655 (4)	0.82196 (5)	0.01345 (8)
C2	0.22987 (10)	0.38609 (5)	0.70430 (5)	0.01411 (8)
C3	0.04598 (12)	0.43527 (5)	0.64009 (6)	0.01785 (10)
H3	0.024785	0.439826	0.561371	0.021*
C4	-0.10516 (12)	0.47734 (5)	0.69429 (7)	0.01963 (11)
H4	-0.227956	0.510676	0.652367	0.024*
C5	-0.07114 (12)	0.46915 (5)	0.81243 (7)	0.01897 (11)
H5	-0.171888	0.497917	0.848747	0.023*
C6	0.11003 (11)	0.41894 (5)	0.87719 (6)	0.01672 (9)
H6	0.129605	0.413606	0.955755	0.020*
C7	0.39425 (10)	0.34091 (5)	0.64974 (5)	0.01428 (8)
C8	0.72947 (9)	0.24140 (4)	0.70329 (5)	0.01212 (7)
C9	0.76909 (10)	0.23588 (5)	0.59317 (5)	0.01581 (9)
H9	0.674954	0.268736	0.534047	0.019*
C10	1.07923 (10)	0.13875 (5)	0.65417 (6)	0.01567 (9)
H10	1.197223	0.104522	0.637531	0.019*
C11	1.05314 (11)	0.14100 (5)	0.76542 (6)	0.01576 (9)
H11	1.152740	0.108503	0.822798	0.019*
C12	0.87733 (10)	0.19211 (5)	0.79026 (5)	0.01420 (8)
H12	0.857647	0.193657	0.864376	0.017*
N1	0.55251 (9)	0.29334 (4)	0.72854 (4)	0.01310 (7)
N2	0.93777 (10)	0.18491 (4)	0.57066 (5)	0.01584 (8)
O1	0.38464 (10)	0.34697 (5)	0.54659 (4)	0.02162 (10)
Se1	0.51666 (2)	0.30054 (2)	0.88714 (2)	0.01258 (1)

*Atomic displacement parameters ( $\text{\AA}^2$ )*

	$U^{11}$	$U^{22}$	$U^{33}$	$U^{12}$	$U^{13}$	$U^{23}$
C1	0.01388 (18)	0.0148 (2)	0.01338 (19)	-0.00130 (15)	0.00657 (15)	-0.00112 (15)
C2	0.01445 (18)	0.0160 (2)	0.01307 (19)	0.00038 (16)	0.00561 (15)	-0.00028 (16)
C3	0.0185 (2)	0.0189 (3)	0.0166 (2)	0.00339 (19)	0.00498 (18)	0.00089 (19)
C4	0.0189 (2)	0.0183 (3)	0.0226 (3)	0.00408 (19)	0.0068 (2)	0.0003 (2)
C5	0.0188 (2)	0.0173 (3)	0.0235 (3)	0.00215 (19)	0.0105 (2)	-0.0017 (2)
C6	0.0176 (2)	0.0180 (2)	0.0172 (2)	0.00016 (18)	0.00939 (18)	-0.00212 (18)
C7	0.01411 (18)	0.0193 (2)	0.01015 (17)	0.00110 (16)	0.00421 (14)	-0.00046 (16)
C8	0.01216 (17)	0.0159 (2)	0.00940 (16)	-0.00061 (14)	0.00477 (13)	-0.00053 (14)

C9	0.0155 (2)	0.0232 (3)	0.01025 (18)	0.00377 (18)	0.00613 (15)	0.00085 (17)
C10	0.0151 (2)	0.0182 (2)	0.0149 (2)	0.00194 (17)	0.00587 (16)	0.00007 (18)
C11	0.0157 (2)	0.0182 (2)	0.0136 (2)	0.00178 (17)	0.00384 (16)	0.00163 (17)
C12	0.01507 (19)	0.0179 (2)	0.01033 (17)	0.00031 (16)	0.00445 (14)	0.00064 (15)
N1	0.01263 (15)	0.0189 (2)	0.00877 (14)	0.00072 (13)	0.00457 (11)	−0.00021 (13)
N2	0.01594 (18)	0.0218 (2)	0.01158 (17)	0.00286 (15)	0.00685 (14)	0.00052 (15)
O1	0.0222 (2)	0.0338 (3)	0.00945 (15)	0.00891 (19)	0.00474 (14)	0.00144 (17)
Se1	0.01163 (2)	0.01794 (3)	0.00946 (2)	−0.00148 (2)	0.00507 (1)	−0.00106 (2)

*Geometric parameters (Å, °)*

C1—C2	1.3927 (9)	C8—N1	1.4007 (7)
C1—C6	1.4023 (8)	C8—C12	1.4009 (9)
C1—Se1	1.9037 (6)	C8—C9	1.4073 (8)
C2—C3	1.3936 (9)	C9—N2	1.3388 (8)
C2—C7	1.4715 (8)	C9—H9	0.9300
C3—C4	1.3863 (10)	C10—N2	1.3354 (9)
C3—H3	0.9300	C10—C11	1.3885 (9)
C4—C5	1.3959 (11)	C10—H10	0.9300
C4—H4	0.9300	C11—C12	1.3867 (9)
C5—C6	1.3925 (10)	C11—H11	0.9300
C5—H5	0.9300	C12—H12	0.9300
C6—H6	0.9300	N1—Se1	1.9788 (5)
C7—O1	1.2349 (8)	Se1—N2 <sup>i</sup>	2.3831 (6)
C7—N1	1.3653 (8)		
C2—C1—C6	119.37 (6)	N1—C8—C9	123.19 (5)
C2—C1—Se1	112.57 (4)	C12—C8—C9	117.09 (5)
C6—C1—Se1	128.04 (5)	N2—C9—C8	122.20 (6)
C1—C2—C3	121.26 (6)	N2—C9—H9	118.9
C1—C2—C7	117.65 (5)	C8—C9—H9	118.9
C3—C2—C7	121.09 (6)	N2—C10—C11	121.12 (6)
C4—C3—C2	119.59 (7)	N2—C10—H10	119.4
C4—C3—H3	120.2	C11—C10—H10	119.4
C2—C3—H3	120.2	C12—C11—C10	119.44 (6)
C3—C4—C5	119.31 (7)	C12—C11—H11	120.3
C3—C4—H4	120.3	C10—C11—H11	120.3
C5—C4—H4	120.3	C11—C12—C8	119.76 (5)
C6—C5—C4	121.58 (6)	C11—C12—H12	120.1
C6—C5—H5	119.2	C8—C12—H12	120.1
C4—C5—H5	119.2	C7—N1—C8	124.50 (5)
C5—C6—C1	118.88 (6)	C7—N1—Se1	115.23 (4)
C5—C6—H6	120.6	C8—N1—Se1	120.27 (4)
C1—C6—H6	120.6	C10—N2—C9	120.38 (5)
O1—C7—N1	126.47 (6)	C1—Se1—N1	83.97 (2)
O1—C7—C2	122.98 (6)	C1—Se1—N2 <sup>i</sup>	90.65 (2)
N1—C7—C2	110.55 (5)	N1—Se1—N2 <sup>i</sup>	174.44 (2)
N1—C8—C12	119.72 (5)		



C6—C1—C2—C3	-1.39 (10)	C12—C8—C9—N2	1.01 (10)
Se1—C1—C2—C3	176.78 (5)	N2—C10—C11—C12	-0.06 (11)
C6—C1—C2—C7	179.72 (6)	C10—C11—C12—C8	-0.52 (10)
Se1—C1—C2—C7	-2.11 (7)	N1—C8—C12—C11	-179.72 (6)
C1—C2—C3—C4	1.42 (11)	C9—C8—C12—C11	0.06 (9)
C7—C2—C3—C4	-179.73 (7)	O1—C7—N1—C8	-1.40 (11)
C2—C3—C4—C5	-0.42 (11)	C2—C7—N1—C8	178.69 (6)
C3—C4—C5—C6	-0.60 (12)	O1—C7—N1—Se1	179.21 (6)
C4—C5—C6—C1	0.63 (11)	C2—C7—N1—Se1	-0.70 (7)
C2—C1—C6—C5	0.36 (10)	C12—C8—N1—C7	-177.43 (6)
Se1—C1—C6—C5	-177.50 (5)	C9—C8—N1—C7	2.81 (10)
C1—C2—C7—O1	-178.07 (7)	C12—C8—N1—Se1	1.93 (8)
C3—C2—C7—O1	3.03 (11)	C9—C8—N1—Se1	-177.84 (5)
C1—C2—C7—N1	1.84 (8)	C11—C10—N2—C9	1.12 (11)
C3—C2—C7—N1	-177.05 (6)	C8—C9—N2—C10	-1.62 (11)
N1—C8—C9—N2	-179.21 (6)		

Symmetry code: (i)  $x-1/2, -y+1/2, z+1/2$ .

### 1-Methyl-3-(3-oxo-2,3-dihydro-1,2-benzoselenazol-2-yl)pyridin-1-ium iodide (2-Melodide)

#### Crystal data

$C_{13}H_{11}N_2OSe^+I^-$

$M_r = 417.10$

Triclinic,  $P\bar{1}$

$a = 7.0926$  (1) Å

$b = 8.1329$  (1) Å

$c = 11.8376$  (1) Å

$\alpha = 84.618$  (1)°

$\beta = 82.243$  (1)°

$\gamma = 77.756$  (1)°

$V = 659.70$  (1) Å<sup>3</sup>

$Z = 2$

$F(000) = 396$

$D_x = 2.100$  Mg m<sup>-3</sup>

Mo  $K\alpha$  radiation,  $\lambda = 0.71073$  Å

Cell parameters from 41098 reflections

$\theta = 3.0$ – $51.1$ °

$\mu = 5.18$  mm<sup>-1</sup>

$T = 100$  K

Needle, pale yellow

$0.46 \times 0.06 \times 0.06$  mm

#### Data collection

Rigaku XtaLAB Synergy

diffractometer with a Dualflex HyPix detector

Radiation source: micro-focus sealed X-ray

tube, PhotonJet (Mo) X-ray Source

Mirror monochromator

$\omega$  scans

Absorption correction: gaussian

(CrysAlis PRO; Rigaku OD, 2020)

$T_{\min} = 0.351$ ,  $T_{\max} = 1.000$

90106 measured reflections

14487 independent reflections

12038 reflections with  $I > 2\sigma(I)$

$R_{\text{int}} = 0.055$

$\theta_{\max} = 51.3$ °,  $\theta_{\min} = 2.6$ °

$h = -15 \rightarrow 14$

$k = -17 \rightarrow 17$

$l = -25 \rightarrow 25$

#### Refinement

Refinement on  $F^2$

Least-squares matrix: full

$R[F^2 > 2\sigma(F^2)] = 0.025$

$wR(F^2) = 0.058$

$S = 1.03$

14487 reflections

164 parameters

0 restraints

Hydrogen site location: inferred from neighbouring sites

H-atom parameters constrained

$$w = 1/[\sigma^2(F_o^2) + (0.0245P)^2 + 0.1355P]$$

where  $P = (F_o^2 + 2F_c^2)/3$   
 $(\Delta/\sigma)_{\max} = 0.002$

$$\Delta\rho_{\max} = 1.24 \text{ e } \text{\AA}^{-3}$$

$$\Delta\rho_{\min} = -1.68 \text{ e } \text{\AA}^{-3}$$

*Special details*

**Geometry.** All esds (except the esd in the dihedral angle between two l.s. planes) are estimated using the full covariance matrix. The cell esds are taken into account individually in the estimation of esds in distances, angles and torsion angles; correlations between esds in cell parameters are only used when they are defined by crystal symmetry. An approximate (isotropic) treatment of cell esds is used for estimating esds involving l.s. planes.

*Fractional atomic coordinates and isotropic or equivalent isotropic displacement parameters ( $\text{\AA}^2$ )*

	x	y	z	$U_{\text{iso}}^*/U_{\text{eq}}$
C1	0.71969 (11)	0.39143 (9)	0.29142 (6)	0.01123 (9)
C2	0.79182 (11)	0.27047 (9)	0.37509 (6)	0.01163 (9)
C3	0.84783 (12)	0.09999 (10)	0.35261 (7)	0.01418 (11)
H3	0.896856	0.020353	0.408538	0.017*
C4	0.82960 (14)	0.05080 (10)	0.24616 (8)	0.01636 (12)
H4	0.867026	-0.062081	0.230157	0.020*
C5	0.75461 (14)	0.17186 (10)	0.16295 (7)	0.01619 (12)
H5	0.741347	0.138094	0.092015	0.019*
C6	0.69947 (12)	0.34201 (10)	0.18441 (7)	0.01391 (11)
H6	0.650023	0.421412	0.128477	0.017*
C7	0.81058 (11)	0.32880 (9)	0.48606 (6)	0.01203 (10)
C8	0.75114 (11)	0.59383 (9)	0.57951 (6)	0.01178 (9)
C9	0.80103 (12)	0.51643 (10)	0.68512 (6)	0.01299 (10)
H9	0.837961	0.399652	0.694047	0.016*
C10	0.74033 (13)	0.77936 (11)	0.76744 (7)	0.01612 (12)
H10	0.735208	0.839759	0.831098	0.019*
C11	0.69091 (14)	0.86244 (11)	0.66475 (8)	0.01657 (12)
H11	0.654041	0.979383	0.658758	0.020*
C12	0.69653 (13)	0.77078 (10)	0.57089 (7)	0.01452 (11)
H12	0.663999	0.826640	0.501827	0.017*
C13	0.85437 (14)	0.51910 (13)	0.88179 (7)	0.01801 (13)
H13A	0.841621	0.598010	0.939150	0.027*
H13B	0.987107	0.460330	0.869192	0.027*
H13C	0.772455	0.439539	0.906967	0.027*
N1	0.75451 (10)	0.50151 (8)	0.48588 (5)	0.01178 (9)
N2	0.79575 (11)	0.61060 (9)	0.77410 (6)	0.01368 (9)
O1	0.87084 (11)	0.23384 (8)	0.56671 (6)	0.01728 (10)
Se1	0.66320 (2)	0.61609 (2)	0.33982 (2)	0.01067 (1)
I1	0.52171 (2)	0.78203 (2)	0.12231 (2)	0.01547 (1)

*Atomic displacement parameters ( $\text{\AA}^2$ )*

	$U^{11}$	$U^{22}$	$U^{33}$	$U^{12}$	$U^{13}$	$U^{23}$
C1	0.0120 (2)	0.0097 (2)	0.0121 (2)	-0.00191 (18)	-0.00218 (18)	-0.00070 (17)
C2	0.0119 (2)	0.0101 (2)	0.0125 (2)	-0.00107 (18)	-0.00215 (19)	-0.00056 (17)
C3	0.0153 (3)	0.0105 (2)	0.0166 (3)	-0.0011 (2)	-0.0039 (2)	-0.00062 (19)

C4	0.0197 (3)	0.0108 (2)	0.0193 (3)	-0.0017 (2)	-0.0057 (3)	-0.0029 (2)
C5	0.0203 (3)	0.0126 (2)	0.0166 (3)	-0.0025 (2)	-0.0054 (2)	-0.0032 (2)
C6	0.0170 (3)	0.0120 (2)	0.0134 (2)	-0.0026 (2)	-0.0044 (2)	-0.00111 (19)
C7	0.0124 (3)	0.0111 (2)	0.0116 (2)	-0.00016 (19)	-0.00161 (19)	-0.00025 (17)
C8	0.0113 (2)	0.0126 (2)	0.0110 (2)	-0.00160 (19)	-0.00085 (18)	-0.00113 (18)
C9	0.0137 (3)	0.0141 (2)	0.0108 (2)	-0.0017 (2)	-0.00181 (19)	-0.00129 (18)
C10	0.0169 (3)	0.0169 (3)	0.0148 (3)	-0.0031 (2)	-0.0007 (2)	-0.0047 (2)
C11	0.0192 (3)	0.0135 (3)	0.0170 (3)	-0.0022 (2)	-0.0018 (2)	-0.0038 (2)
C12	0.0165 (3)	0.0127 (2)	0.0140 (3)	-0.0015 (2)	-0.0021 (2)	-0.0013 (2)
C13	0.0197 (3)	0.0234 (4)	0.0113 (2)	-0.0050 (3)	-0.0028 (2)	-0.0005 (2)
N1	0.0138 (2)	0.01025 (19)	0.01058 (19)	-0.00051 (17)	-0.00220 (17)	-0.00022 (15)
N2	0.0135 (2)	0.0166 (2)	0.0111 (2)	-0.0029 (2)	-0.00118 (17)	-0.00226 (17)
O1	0.0227 (3)	0.0130 (2)	0.0137 (2)	0.0029 (2)	-0.0049 (2)	0.00079 (16)
Se1	0.01193 (3)	0.00899 (2)	0.01078 (3)	-0.00127 (2)	-0.00170 (2)	-0.00046 (2)
I1	0.02283 (3)	0.01112 (2)	0.01269 (2)	-0.00161 (2)	-0.00644 (2)	0.00004 (1)

*Geometric parameters (Å, °)*

C1—C2	1.3968 (10)	C8—N1	1.3907 (10)
C1—C6	1.3984 (10)	C8—C9	1.4006 (10)
C1—Se1	1.9108 (7)	C8—C12	1.4065 (11)
C2—C3	1.3993 (11)	C9—N2	1.3514 (10)
C2—C7	1.4695 (11)	C10—N2	1.3430 (12)
C3—C4	1.3875 (12)	C10—C11	1.3848 (13)
C4—C5	1.3999 (12)	C11—C12	1.3866 (12)
C5—C6	1.3936 (11)	C13—N2	1.4784 (11)
C7—O1	1.2339 (9)	N1—Se1	2.0053 (6)
C7—N1	1.3762 (10)	Se1—I1	2.9882 (1)
C2—C1—C6	119.89 (7)	C9—C8—C12	117.39 (7)
C2—C1—Se1	113.17 (5)	N2—C9—C8	120.32 (7)
C6—C1—Se1	126.93 (6)	N2—C10—C11	119.27 (7)
C1—C2—C3	120.80 (7)	C10—C11—C12	119.82 (8)
C1—C2—C7	117.81 (6)	C11—C12—C8	120.40 (8)
C3—C2—C7	121.37 (7)	C7—N1—C8	124.27 (6)
C4—C3—C2	119.42 (7)	C7—N1—Se1	114.94 (5)
C3—C4—C5	119.70 (7)	C8—N1—Se1	120.73 (5)
C6—C5—C4	121.24 (7)	C10—N2—C9	122.78 (7)
C5—C6—C1	118.93 (7)	C10—N2—C13	120.40 (7)
O1—C7—N1	125.66 (7)	C9—N2—C13	116.82 (7)
O1—C7—C2	123.71 (7)	C1—Se1—N1	83.43 (3)
N1—C7—C2	110.63 (6)	C1—Se1—I1	95.85 (2)
N1—C8—C9	122.12 (7)	N1—Se1—I1	178.85 (2)
N1—C8—C12	120.50 (7)		
C6—C1—C2—C3	1.19 (12)	N2—C10—C11—C12	0.90 (14)
Se1—C1—C2—C3	-177.56 (6)	C10—C11—C12—C8	0.34 (13)
C6—C1—C2—C7	179.92 (7)	N1—C8—C12—C11	179.18 (8)

Se1—C1—C2—C7	1.17 (9)	C9—C8—C12—C11	−0.79 (12)
C1—C2—C3—C4	−0.60 (12)	O1—C7—N1—C8	−2.54 (13)
C7—C2—C3—C4	−179.28 (8)	C2—C7—N1—C8	178.26 (7)
C2—C3—C4—C5	−0.34 (13)	O1—C7—N1—Se1	−179.84 (7)
C3—C4—C5—C6	0.70 (14)	C2—C7—N1—Se1	0.97 (8)
C4—C5—C6—C1	−0.11 (13)	C9—C8—N1—C7	−1.69 (12)
C2—C1—C6—C5	−0.83 (12)	C12—C8—N1—C7	178.33 (8)
Se1—C1—C6—C5	177.74 (6)	C9—C8—N1—Se1	175.46 (6)
C1—C2—C7—O1	179.39 (8)	C12—C8—N1—Se1	−4.52 (10)
C3—C2—C7—O1	−1.90 (13)	C11—C10—N2—C9	−1.72 (13)
C1—C2—C7—N1	−1.40 (10)	C11—C10—N2—C13	178.35 (8)
C3—C2—C7—N1	177.32 (7)	C8—C9—N2—C10	1.26 (12)
N1—C8—C9—N2	−179.95 (7)	C8—C9—N2—C13	−178.82 (8)
C12—C8—C9—N2	0.03 (12)		

1-Methyl-3-(3-oxo-2,3-dihydro-1,2-benzoselenazol-2-yl)pyridin-1-ium toluenesulfonate trihydrate (2-Metosylate)

Crystal data

$C_{13}H_{11}N_2OSe^+ \cdot C_7H_7O_3S^- \cdot 3H_2O$

$M_r = 515.43$

Triclinic,  $P\bar{1}$

$a = 6.9412$  (3) Å

$b = 12.1279$  (4) Å

$c = 13.5994$  (3) Å

$\alpha = 70.426$  (3)°

$\beta = 83.774$  (3)°

$\gamma = 83.585$  (3)°

$V = 1068.83$  (7) Å<sup>3</sup>

$Z = 2$

$F(000) = 528$

$D_x = 1.602$  Mg m<sup>−3</sup>

Cu  $K\alpha$  radiation,  $\lambda = 1.54184$  Å

Cell parameters from 5181 reflections

$\theta = 3.5$ – $75.2$ °

$\mu = 3.70$  mm<sup>−1</sup>

$T = 100$  K

Rod, colourless

$0.21 \times 0.03 \times 0.03$  mm

Data collection

Rigaku XtaLAB Synergy  
diffractometer with a Dualflex HyPix detector

Radiation source: micro-focus sealed X-ray  
tube, PhotonJet (Cu) X-ray Source

Mirror monochromator

$\omega$  scans

Absorption correction: multi-scan  
(CrysAlis PRO; Rigaku OD, 2020)

$T_{\min} = 0.668$ ,  $T_{\max} = 1.000$

15253 measured reflections

4435 independent reflections

3777 reflections with  $I > 2\sigma(I)$

$R_{\text{int}} = 0.064$

$\theta_{\max} = 77.1$ °,  $\theta_{\min} = 3.5$ °

$h = -8 \rightarrow 8$

$k = -15 \rightarrow 14$

$l = -17 \rightarrow 12$

Refinement

Refinement on  $F^2$

Least-squares matrix: full

$R[F^2 > 2\sigma(F^2)] = 0.041$

$wR(F^2) = 0.104$

$S = 1.06$

4435 reflections

306 parameters

6 restraints

Hydrogen site location: mixed

H atoms treated by a mixture of independent  
and constrained refinement

$w = 1/[\sigma^2(F_o^2) + (0.0467P)^2 + 0.8165P]$

where  $P = (F_o^2 + 2F_c^2)/3$

$(\Delta/\sigma)_{\max} = 0.002$

$\Delta\rho_{\max} = 0.89$  e Å<sup>−3</sup>

$\Delta\rho_{\min} = -0.66$  e Å<sup>−3</sup>



*Special details*

**Geometry.** All esds (except the esd in the dihedral angle between two l.s. planes) are estimated using the full covariance matrix. The cell esds are taken into account individually in the estimation of esds in distances, angles and torsion angles; correlations between esds in cell parameters are only used when they are defined by crystal symmetry. An approximate (isotropic) treatment of cell esds is used for estimating esds involving l.s. planes.

*Fractional atomic coordinates and isotropic or equivalent isotropic displacement parameters ( $\text{\AA}^2$ )*

	<i>x</i>	<i>y</i>	<i>z</i>	$U_{\text{iso}}^*/U_{\text{eq}}$
C1	0.8190 (4)	0.7622 (3)	0.3959 (2)	0.0168 (6)
C2	0.8275 (4)	0.7065 (3)	0.3204 (2)	0.0159 (6)
C3	0.8578 (5)	0.7701 (3)	0.2146 (2)	0.0188 (6)
H3	0.866644	0.732945	0.164377	0.023*
C4	0.8746 (5)	0.8900 (3)	0.1854 (2)	0.0226 (6)
H4	0.893600	0.933839	0.114989	0.027*
C5	0.8632 (5)	0.9451 (3)	0.2610 (2)	0.0219 (6)
H5	0.874122	1.025597	0.240133	0.026*
C6	0.8358 (4)	0.8819 (3)	0.3673 (2)	0.0181 (6)
H6	0.828948	0.918880	0.417614	0.022*
C7	0.7994 (4)	0.5803 (3)	0.3584 (2)	0.0161 (6)
C8	0.7311 (4)	0.4253 (3)	0.5279 (2)	0.0160 (5)
C9	0.7287 (4)	0.3370 (2)	0.4827 (2)	0.0159 (5)
H9	0.748075	0.354387	0.410553	0.019*
C10	0.6692 (4)	0.1952 (3)	0.6505 (2)	0.0193 (6)
H10	0.648572	0.118029	0.690666	0.023*
C11	0.6709 (5)	0.2800 (3)	0.6974 (2)	0.0196 (6)
H11	0.651838	0.259970	0.769823	0.023*
C12	0.7009 (4)	0.3946 (3)	0.6369 (2)	0.0180 (6)
H12	0.700960	0.451510	0.668790	0.022*
C13	0.6874 (5)	0.1362 (3)	0.4938 (2)	0.0219 (6)
H13A	0.558950	0.141560	0.471721	0.033*
H13B	0.716429	0.059415	0.542568	0.033*
H13C	0.780073	0.149830	0.434065	0.033*
C14	0.6943 (5)	0.6893 (3)	0.7742 (2)	0.0164 (6)
C15	0.7931 (5)	0.5789 (3)	0.8140 (2)	0.0184 (6)
H15	0.928204	0.570166	0.806274	0.022*
C16	0.6882 (5)	0.4822 (3)	0.8651 (2)	0.0189 (6)
H16	0.753989	0.408680	0.892389	0.023*
C17	0.4847 (5)	0.4934 (3)	0.8764 (2)	0.0173 (6)
C18	0.3897 (5)	0.6043 (3)	0.8350 (2)	0.0198 (6)
H18	0.254535	0.613102	0.841374	0.024*
C19	0.4926 (4)	0.7019 (3)	0.7845 (2)	0.0174 (6)
H19	0.426845	0.775505	0.757722	0.021*
C20	0.3731 (5)	0.3878 (3)	0.9329 (2)	0.0226 (6)
H20A	0.236385	0.411220	0.934341	0.034*
H20B	0.411240	0.353814	1.003290	0.034*
H20C	0.400585	0.330948	0.897251	0.034*
N1	0.7666 (4)	0.5400 (2)	0.46661 (19)	0.0150 (5)

N2	0.6979 (4)	0.2264 (2)	0.54526 (19)	0.0171 (5)
O1	0.8011 (3)	0.51913 (19)	0.30289 (16)	0.0212 (5)
O2	0.8222 (4)	0.82842 (19)	0.59419 (16)	0.0232 (5)
O3	0.7166 (3)	0.91295 (18)	0.72943 (16)	0.0204 (4)
O4	1.0197 (3)	0.78786 (19)	0.74049 (18)	0.0227 (5)
O5	0.6998 (4)	0.9143 (2)	0.93465 (18)	0.0248 (5)
O6	1.0582 (4)	0.7845 (2)	0.96242 (19)	0.0285 (5)
O7	0.6591 (4)	1.1350 (2)	0.95412 (18)	0.0266 (5)
S1	0.82392 (10)	0.81327 (6)	0.70567 (5)	0.01569 (16)
Se1	0.77888 (4)	0.65552 (3)	0.53384 (2)	0.01444 (11)
H5A	0.684 (5)	0.917 (3)	0.8752 (13)	0.015 (9)*
H5B	0.724 (12)	0.976 (4)	0.941 (6)	0.10 (3)*
H6A	1.070 (8)	0.770 (5)	0.907 (2)	0.049 (15)*
H6B	0.947 (4)	0.813 (6)	0.968 (5)	0.08 (2)*
H7A	0.746 (5)	1.159 (4)	0.976 (4)	0.045 (14)*
H7B	0.555 (4)	1.126 (6)	0.989 (4)	0.063 (18)*

*Atomic displacement parameters (Å<sup>2</sup>)*

	$U^{11}$	$U^{22}$	$U^{33}$	$U^{12}$	$U^{13}$	$U^{23}$
C1	0.0142 (14)	0.0148 (13)	0.0190 (14)	0.0012 (11)	-0.0031 (11)	-0.0026 (11)
C2	0.0153 (14)	0.0128 (13)	0.0187 (14)	-0.0014 (11)	-0.0013 (11)	-0.0039 (11)
C3	0.0216 (15)	0.0163 (14)	0.0179 (14)	-0.0027 (12)	-0.0021 (11)	-0.0041 (11)
C4	0.0264 (16)	0.0223 (15)	0.0158 (14)	-0.0061 (13)	-0.0031 (12)	0.0000 (12)
C5	0.0285 (17)	0.0139 (14)	0.0207 (15)	-0.0033 (12)	-0.0043 (12)	-0.0010 (12)
C6	0.0182 (14)	0.0152 (14)	0.0195 (14)	-0.0008 (11)	-0.0028 (11)	-0.0036 (11)
C7	0.0157 (14)	0.0132 (13)	0.0160 (13)	0.0022 (11)	-0.0024 (11)	-0.0012 (11)
C8	0.0130 (13)	0.0146 (13)	0.0198 (14)	-0.0015 (11)	-0.0033 (11)	-0.0040 (11)
C9	0.0225 (15)	0.0089 (12)	0.0132 (13)	0.0002 (11)	-0.0018 (11)	0.0003 (10)
C10	0.0176 (14)	0.0155 (14)	0.0198 (14)	-0.0013 (11)	0.0009 (11)	0.0001 (11)
C11	0.0180 (15)	0.0178 (14)	0.0190 (14)	-0.0014 (12)	-0.0006 (11)	-0.0011 (12)
C12	0.0184 (14)	0.0158 (14)	0.0172 (14)	-0.0009 (11)	-0.0018 (11)	-0.0022 (11)
C13	0.0263 (16)	0.0158 (14)	0.0227 (15)	-0.0042 (12)	0.0009 (12)	-0.0050 (12)
C14	0.0230 (15)	0.0134 (13)	0.0122 (12)	-0.0031 (11)	-0.0021 (10)	-0.0028 (10)
C15	0.0198 (15)	0.0157 (14)	0.0188 (13)	-0.0006 (11)	-0.0020 (11)	-0.0045 (11)
C16	0.0261 (16)	0.0128 (13)	0.0154 (13)	0.0002 (12)	-0.0015 (11)	-0.0020 (11)
C17	0.0232 (15)	0.0169 (14)	0.0121 (12)	-0.0036 (12)	0.0013 (11)	-0.0053 (11)
C18	0.0192 (15)	0.0194 (15)	0.0201 (14)	-0.0027 (12)	-0.0007 (11)	-0.0052 (12)
C19	0.0198 (15)	0.0118 (13)	0.0179 (13)	0.0019 (11)	-0.0016 (11)	-0.0022 (11)
C20	0.0275 (17)	0.0191 (15)	0.0209 (15)	-0.0062 (13)	-0.0013 (12)	-0.0047 (12)
N1	0.0166 (12)	0.0116 (11)	0.0154 (11)	0.0022 (9)	-0.0024 (9)	-0.0031 (9)
N2	0.0148 (12)	0.0150 (12)	0.0193 (12)	-0.0010 (9)	-0.0007 (9)	-0.0030 (10)
O1	0.0329 (13)	0.0176 (10)	0.0149 (10)	-0.0048 (9)	-0.0016 (9)	-0.0069 (8)
O2	0.0350 (13)	0.0189 (11)	0.0143 (10)	-0.0087 (9)	0.0027 (9)	-0.0030 (8)
O3	0.0271 (12)	0.0128 (10)	0.0201 (10)	-0.0005 (9)	-0.0003 (9)	-0.0044 (8)
O4	0.0208 (11)	0.0173 (10)	0.0283 (11)	-0.0030 (9)	-0.0028 (9)	-0.0043 (9)
O5	0.0304 (13)	0.0247 (12)	0.0214 (11)	-0.0006 (10)	-0.0018 (9)	-0.0107 (9)
O6	0.0285 (14)	0.0281 (13)	0.0286 (12)	0.0033 (11)	-0.0054 (10)	-0.0098 (10)

O7	0.0292 (14)	0.0250 (12)	0.0237 (12)	-0.0046 (11)	-0.0005 (10)	-0.0051 (10)
S1	0.0195 (4)	0.0121 (3)	0.0146 (3)	-0.0020 (3)	0.0004 (3)	-0.0036 (2)
Se1	0.01618 (17)	0.01222 (16)	0.01383 (16)	-0.00101 (11)	-0.00065 (10)	-0.00301 (11)

*Geometric parameters (Å, °)*

C1—C6	1.387 (4)	C13—H13C	0.9600
C1—C2	1.398 (4)	C14—C19	1.388 (4)
C1—Se1	1.901 (3)	C14—C15	1.395 (4)
C2—C3	1.391 (4)	C14—S1	1.767 (3)
C2—C7	1.471 (4)	C15—C16	1.387 (4)
C3—C4	1.389 (4)	C15—H15	0.9300
C3—H3	0.9300	C16—C17	1.400 (4)
C4—C5	1.392 (5)	C16—H16	0.9300
C4—H4	0.9300	C17—C18	1.392 (4)
C5—C6	1.395 (4)	C17—C20	1.505 (4)
C5—H5	0.9300	C18—C19	1.386 (4)
C6—H6	0.9300	C18—H18	0.9300
C7—O1	1.221 (4)	C19—H19	0.9300
C7—N1	1.388 (4)	C20—H20A	0.9600
C8—N1	1.395 (4)	C20—H20B	0.9600
C8—C12	1.400 (4)	C20—H20C	0.9600
C8—C9	1.404 (4)	N1—Se1	1.926 (2)
C9—N2	1.352 (4)	O2—S1	1.466 (2)
C9—H9	0.9300	O3—S1	1.459 (2)
C10—N2	1.350 (4)	O4—S1	1.454 (2)
C10—C11	1.382 (4)	O5—H5A	0.816 (10)
C10—H10	0.9300	O5—H5B	0.820 (10)
C11—C12	1.383 (4)	O6—H6A	0.819 (10)
C11—H11	0.9300	O6—H6B	0.820 (10)
C12—H12	0.9300	O7—H7A	0.819 (10)
C13—N2	1.494 (4)	O7—H7B	0.820 (10)
C13—H13A	0.9600	O2—Se1	2.553 (2)
C13—H13B	0.9600		
C6—C1—C2	121.1 (3)	C19—C14—C15	120.2 (3)
C6—C1—Se1	126.9 (2)	C19—C14—S1	119.3 (2)
C2—C1—Se1	112.0 (2)	C15—C14—S1	120.4 (2)
C3—C2—C1	120.4 (3)	C16—C15—C14	119.4 (3)
C3—C2—C7	122.7 (3)	C16—C15—H15	120.3
C1—C2—C7	116.9 (3)	C14—C15—H15	120.3
C4—C3—C2	118.8 (3)	C15—C16—C17	121.1 (3)
C4—C3—H3	120.6	C15—C16—H16	119.5
C2—C3—H3	120.6	C17—C16—H16	119.5
C3—C4—C5	120.4 (3)	C18—C17—C16	118.4 (3)
C3—C4—H4	119.8	C18—C17—C20	121.2 (3)
C5—C4—H4	119.8	C16—C17—C20	120.4 (3)
C4—C5—C6	121.2 (3)	C19—C18—C17	121.2 (3)

C4—C5—H5	119.4	C19—C18—H18	119.4
C6—C5—H5	119.4	C17—C18—H18	119.4
C1—C6—C5	118.0 (3)	C18—C19—C14	119.7 (3)
C1—C6—H6	121.0	C18—C19—H19	120.2
C5—C6—H6	121.0	C14—C19—H19	120.2
O1—C7—N1	124.3 (3)	C17—C20—H20A	109.5
O1—C7—C2	125.0 (3)	C17—C20—H20B	109.5
N1—C7—C2	110.7 (2)	H20A—C20—H20B	109.5
N1—C8—C12	120.6 (3)	C17—C20—H20C	109.5
N1—C8—C9	121.2 (3)	H20A—C20—H20C	109.5
C12—C8—C9	118.2 (3)	H20B—C20—H20C	109.5
N2—C9—C8	119.3 (3)	C7—N1—C8	125.7 (2)
N2—C9—H9	120.4	C7—N1—Se1	115.07 (19)
C8—C9—H9	120.4	C8—N1—Se1	119.21 (19)
N2—C10—C11	118.8 (3)	C10—N2—C9	123.4 (3)
N2—C10—H10	120.6	C10—N2—C13	119.0 (3)
C11—C10—H10	120.6	C9—N2—C13	117.6 (2)
C10—C11—C12	120.2 (3)	H5A—O5—H5B	116 (6)
C10—C11—H11	119.9	H6A—O6—H6B	106 (6)
C12—C11—H11	119.9	H7A—O7—H7B	118 (6)
C11—C12—C8	120.3 (3)	O4—S1—O3	113.77 (13)
C11—C12—H12	119.9	O4—S1—O2	112.06 (14)
C8—C12—H12	119.9	O3—S1—O2	110.46 (13)
N2—C13—H13A	109.5	O4—S1—C14	107.19 (13)
N2—C13—H13B	109.5	O3—S1—C14	106.57 (14)
H13A—C13—H13B	109.5	O2—S1—C14	106.30 (13)
N2—C13—H13C	109.5	C1—Se1—N1	85.33 (12)
H13A—C13—H13C	109.5	O2—Se1—N1	170.57 (10)
H13B—C13—H13C	109.5		
C6—C1—C2—C3	1.5 (4)	C15—C16—C17—C20	-179.4 (3)
Se1—C1—C2—C3	-179.4 (2)	C16—C17—C18—C19	-0.5 (4)
C6—C1—C2—C7	-177.3 (3)	C20—C17—C18—C19	178.9 (3)
Se1—C1—C2—C7	1.7 (3)	C17—C18—C19—C14	0.4 (4)
C1—C2—C3—C4	-1.5 (4)	C15—C14—C19—C18	0.3 (4)
C7—C2—C3—C4	177.3 (3)	S1—C14—C19—C18	177.8 (2)
C2—C3—C4—C5	0.6 (5)	O1—C7—N1—C8	0.0 (5)
C3—C4—C5—C6	0.3 (5)	C2—C7—N1—C8	178.9 (3)
C2—C1—C6—C5	-0.6 (5)	O1—C7—N1—Se1	178.5 (2)
Se1—C1—C6—C5	-179.4 (2)	C2—C7—N1—Se1	-2.7 (3)
C4—C5—C6—C1	-0.4 (5)	C12—C8—N1—C7	179.7 (3)
C3—C2—C7—O1	0.6 (5)	C9—C8—N1—C7	1.0 (4)
C1—C2—C7—O1	179.4 (3)	C12—C8—N1—Se1	1.3 (4)
C3—C2—C7—N1	-178.2 (3)	C9—C8—N1—Se1	-177.4 (2)
C1—C2—C7—N1	0.6 (4)	C11—C10—N2—C9	0.0 (4)
N1—C8—C9—N2	178.6 (3)	C11—C10—N2—C13	-177.3 (3)
C12—C8—C9—N2	-0.1 (4)	C8—C9—N2—C10	-0.1 (4)
N2—C10—C11—C12	0.3 (4)	C8—C9—N2—C13	177.3 (3)



C10—C11—C12—C8	−0.5 (5)	C19—C14—S1—O4	158.2 (2)
N1—C8—C12—C11	−178.3 (3)	C15—C14—S1—O4	−24.3 (3)
C9—C8—C12—C11	0.4 (4)	C19—C14—S1—O3	36.0 (3)
C19—C14—C15—C16	−0.8 (4)	C15—C14—S1—O3	−146.4 (2)
S1—C14—C15—C16	−178.3 (2)	C19—C14—S1—O2	−81.8 (2)
C14—C15—C16—C17	0.7 (4)	C15—C14—S1—O2	95.7 (2)
C15—C16—C17—C18	−0.1 (4)		

Hydrogen-bond geometry (Å, °)

<i>D</i> —H... <i>A</i>	<i>D</i> —H	H... <i>A</i>	<i>D</i> ... <i>A</i>	<i>D</i> —H... <i>A</i>
C6—H6...O2	0.93	2.28	2.925 (4)	126
C9—H9...O1	0.93	2.09	2.734 (4)	125
C10—H10...O3 <sup>i</sup>	0.93	2.37	3.216 (4)	152
C11—H11...O7 <sup>i</sup>	0.93	2.46	3.338 (4)	158
C12—H12...Se1	0.93	2.61	3.085 (3)	112
C13—H13B...O3 <sup>i</sup>	0.96	2.57	3.442 (4)	152
C13—H13C...O4 <sup>ii</sup>	0.96	2.54	3.490 (4)	170
C15—H15...O1 <sup>ii</sup>	0.93	2.63	3.379 (4)	138
O5—H5A...O3	0.82 (1)	1.99 (1)	2.786 (3)	166 (4)
O5—H5A...S1	0.82 (1)	3.01 (2)	3.698 (2)	144 (3)
O5—H5B...O7	0.82 (1)	1.99 (4)	2.758 (3)	155 (8)
O6—H6A...O4	0.82 (1)	2.27 (2)	3.045 (3)	159 (5)
O6—H6B...O5	0.82 (1)	1.99 (2)	2.782 (4)	162 (7)
O7—H7A...O6 <sup>iii</sup>	0.82 (1)	1.97 (1)	2.783 (4)	176 (5)
O7—H7B...O5 <sup>iv</sup>	0.82 (1)	1.97 (1)	2.786 (4)	172 (6)

Symmetry codes: (i)  $x, y-1, z$ ; (ii)  $-x+2, -y+1, -z+1$ ; (iii)  $-x+2, -y+2, -z+2$ ; (iv)  $-x+1, -y+2, -z+2$ .

(2-multipole)

Crystal data

$C_{12}H_8N_2OSe$

$M_r = 275.16$

Monoclinic,  $P2_1/n$

$a = 6.1074$  (1) Å

$b = 14.2227$  (3) Å

$c = 12.0621$  (2) Å

$\beta = 103.588$  (2)°

$V = 1018.43$  (3) Å<sup>3</sup>

$Z = 4$

$F(000) = 544.0$

$D_x = 1.795$  Mg m<sup>−3</sup>

Mo  $K\alpha$  radiation,  $\lambda = 0.71073$  Å

Cell parameters from 30292 reflections

$\theta = 3.3$ – $56.9$ °

$\mu = 3.66$  mm<sup>−1</sup>

$T = 100$  K

Plate, colourless

$0.48 \times 0.15 \times 0.05$  mm

Data collection

Rigaku XtaLAB Synergy

diffractometer with a Dualflex HyPix detector

Detector resolution: 10.0000 pixels mm<sup>−1</sup>

$\omega$  scans

Absorption correction: gaussian

(CrysAlis PRO; Rigaku OD, 2020)

$T_{\min} = 0.147$ ,  $T_{\max} = 1.000$

97589 measured reflections

7174 independent reflections

6298 reflections with  $I \geq 2\sigma(I)$

$R_{\text{int}} = 0.044$

$\theta_{\max} = 42.5$ °,  $\theta_{\min} = 2.3$ °

$h = -11 \rightarrow 11$

$k = 0 \rightarrow 27$

$l = 0 \rightarrow 22$

Refinement

Refinement on  $F^2$

Least-squares matrix: full

$R[F^2 > 2\sigma(F^2)] = 0.016$

$wR(F^2) = 0.023$

$S = 1.07$

7174 reflections

496 parameters

22 restraints

Primary atom site location: dual

Hydrogen site location: difference Fourier map

All H-atom parameters refined

Weighting scheme based on measured s.u.'s

$(\Delta/\sigma)_{\max} = 0.002$

$\Delta\rho_{\max} = 0.43 \text{ e } \text{\AA}^{-3}$

$\Delta\rho_{\min} = -0.41 \text{ e } \text{\AA}^{-3}$

Extinction correction: Isotropic Gaussian

Extinction coefficient: 0.04936

Special details

**Refinement.** Refinement of  $F^2$  against reflections. The threshold expression of  $F^2 > 2\sigma(F^2)$  is used for calculating R-factors(gt) and is not relevant to the choice of reflections for refinement. R-factors based on  $F^2$  are statistically about twice as large as those based on  $F$ , and R-factors based on ALL data will be even larger.

Fractional atomic coordinates and isotropic or equivalent isotropic displacement parameters ( $\text{\AA}^2$ )

	<i>x</i>	<i>y</i>	<i>z</i>	$U_{\text{iso}}^*/U_{\text{eq}}$
Se1	0.51663 (2)	0.699436 (9)	0.887178 (14)	0.012113 (6)
O1	0.38467 (14)	0.65312 (7)	0.54626 (9)	0.02111 (5)
N1	0.55245 (7)	0.70667 (3)	0.72847 (4)	0.01270 (4)
N2	0.9374 (4)	0.81528 (12)	0.5706 (2)	0.01575 (5)
C1	0.26250 (8)	0.62347 (3)	0.82216 (5)	0.01323 (5)
C2	0.2306 (2)	0.61392 (9)	0.70464 (16)	0.01386 (5)
C3	0.0461 (2)	0.56468 (8)	0.63997 (11)	0.01781 (5)
H3	0.0226 (10)	0.5612 (6)	0.5484 (5)	0.0216 (2)*
C4	-0.10556 (8)	0.52248 (4)	0.69409 (6)	0.01953 (6)
H4	-0.2515 (10)	0.4851 (6)	0.6461 (4)	0.0239 (3)*
C5	-0.0708 (2)	0.53071 (8)	0.81292 (14)	0.01867 (5)
H5	-0.1916 (10)	0.4989 (6)	0.8547 (4)	0.0234 (3)*
C6	0.11028 (8)	0.58119 (3)	0.87722 (5)	0.01661 (5)
H6	0.1343 (10)	0.5872 (6)	0.9687 (5)	0.0210 (2)*
C7	0.3944 (3)	0.65887 (10)	0.65014 (18)	0.01399 (5)
C8	0.7294 (2)	0.75854 (9)	0.70353 (15)	0.01191 (5)
C9	0.7686 (2)	0.76403 (10)	0.59294 (15)	0.01553 (5)
H9	0.6628 (15)	0.7278 (7)	0.5210 (8)	0.0192 (2)*
C10	1.0790 (3)	0.86130 (10)	0.65400 (18)	0.01554 (5)
H10	1.2121 (12)	0.9010 (6)	0.6304 (9)	0.0191 (2)*
C11	1.05275 (17)	0.85906 (7)	0.76568 (12)	0.01566 (5)
H11	1.1681 (11)	0.8975 (5)	0.8323 (5)	0.0189 (2)*
C12	0.87661 (19)	0.80772 (8)	0.79030 (12)	0.01403 (5)
H12	0.8535 (10)	0.8055 (5)	0.8764 (5)	0.01711 (19)*

Atomic displacement parameters ( $\text{\AA}^2$ )

	$U^{11}$	$U^{22}$	$U^{33}$	$U^{12}$	$U^{13}$	$U^{23}$
Se1	0.011160 (19)	0.01721 (2)	0.00917 (2)	0.001535 (16)	0.004801 (14)	0.001001 (17)
O1	0.02195 (16)	0.0330 (2)	0.00884 (17)	-0.00904 (15)	0.00461 (11)	-0.00182 (13)
N1	0.01210 (12)	0.01846 (18)	0.00852 (15)	-0.00141 (14)	0.00441 (11)	-0.00004 (13)

N2	0.01573 (16)	0.0220 (2)	0.0113 (2)	-0.0039 (2)	0.00676 (15)	-0.00071 (15)
C1	0.01383 (15)	0.0150 (2)	0.0125 (2)	0.00056 (16)	0.00633 (14)	0.00108 (14)
C2	0.01395 (14)	0.0162 (2)	0.0124 (2)	-0.00123 (16)	0.00509 (14)	0.00007 (14)
C3	0.01808 (15)	0.0191 (2)	0.0168 (2)	-0.00429 (16)	0.00514 (14)	-0.00106 (15)
C4	0.01879 (16)	0.0188 (2)	0.0219 (2)	-0.00492 (15)	0.00673 (15)	-0.00043 (16)
C5	0.01847 (16)	0.0175 (2)	0.0226 (2)	-0.00288 (15)	0.00981 (15)	0.00125 (15)
C6	0.01754 (16)	0.0181 (2)	0.0168 (2)	-0.00100 (16)	0.00939 (15)	0.00156 (15)
C7	0.01419 (15)	0.0191 (2)	0.0094 (2)	-0.00185 (16)	0.00437 (14)	0.00024 (15)
C8	0.01199 (13)	0.01593 (18)	0.00883 (18)	0.00008 (15)	0.00445 (12)	0.00001 (14)
C9	0.01554 (15)	0.0228 (2)	0.00965 (19)	-0.00412 (17)	0.00583 (13)	-0.00099 (15)
C10	0.01520 (15)	0.0185 (2)	0.0140 (2)	-0.00282 (18)	0.00573 (15)	-0.00048 (16)
C11	0.01563 (14)	0.01821 (19)	0.01338 (19)	-0.00267 (14)	0.00388 (12)	-0.00176 (14)
C12	0.01492 (13)	0.0182 (2)	0.00963 (17)	-0.00090 (15)	0.00421 (12)	-0.00094 (14)

*Geometric parameters (Å, °)*

Se1—N1	1.9799 (5)	C4—C5	1.4037 (16)
Se1—C1	1.9025 (6)	C4—H4	1.081 (5)
O1—C7	1.243 (2)	C5—C6	1.3915 (15)
N1—C7	1.363 (2)	C5—H5	1.085 (5)
N1—C8	1.3982 (17)	C6—H6	1.082 (6)
N2—C10	1.334 (3)	C8—C9	1.412 (2)
N2—C9	1.341 (2)	C8—C12	1.3968 (19)
C1—C2	1.3914 (18)	C9—H9	1.083 (6)
C1—C6	1.3989 (7)	C10—C11	1.394 (2)
C2—C7	1.467 (2)	C10—H10	1.082 (6)
C2—C3	1.399 (2)	C11—C12	1.389 (2)
C3—C4	1.3886 (12)	C11—H11	1.084 (5)
C3—H3	1.081 (5)	C12—H12	1.081 (5)
N1—Se1—C1	84.01 (2)	C1—C6—H6	120.3 (3)
Se1—N1—C7	115.04 (9)	C5—C6—H6	120.6 (3)
Se1—N1—C8	120.13 (7)	O1—C7—N1	126.16 (14)
C7—N1—C8	124.83 (11)	O1—C7—C2	123.16 (14)
C10—N2—C9	120.50 (18)	N1—C7—C2	110.68 (13)
Se1—C1—C2	112.38 (8)	N1—C8—C9	122.93 (12)
Se1—C1—C6	128.12 (4)	N1—C8—C12	119.80 (11)
C2—C1—C6	119.48 (8)	C9—C8—C12	117.26 (13)
C1—C2—C7	117.86 (13)	N2—C9—C8	121.96 (15)
C1—C2—C3	121.24 (12)	N2—C9—H9	116.0 (6)
C7—C2—C3	120.89 (13)	C8—C9—H9	122.0 (6)
C2—C3—C4	119.56 (10)	N2—C10—C11	121.11 (16)
C2—C3—H3	119.3 (3)	N2—C10—H10	116.9 (5)
C4—C3—H3	121.2 (3)	C11—C10—H10	122.0 (5)
C3—C4—C5	119.10 (8)	C10—C11—C12	119.29 (11)
C3—C4—H4	121.2 (3)	C10—C11—H11	120.2 (3)
C5—C4—H4	119.7 (3)	C12—C11—H11	120.5 (3)
C6—C5—C4	121.46 (9)	C8—C12—C11	119.85 (11)

C6—C5—H5	119.6 (3)	C8—C12—H12	119.9 (3)
C4—C5—H5	118.9 (3)	C11—C12—H12	120.2 (3)
C1—C6—C5	119.14 (6)		
Se1—N1—C7—O1	-179.48 (8)	C2—C7—N1—C8	-178.73 (12)
Se1—N1—C7—C2	0.88 (6)	C2—C3—C4—C5	0.37 (12)
Se1—N1—C8—C9	177.90 (7)	C2—C3—C4—H4	178.8 (6)
Se1—N1—C8—C12	-2.03 (7)	C3—C2—C1—C6	1.53 (11)
Se1—C1—C2—C7	2.05 (6)	C3—C4—C5—C6	0.87 (11)
Se1—C1—C2—C3	-176.72 (7)	C3—C4—C5—H5	178.7 (6)
Se1—C1—C6—C5	177.66 (7)	H3—C3—C2—C7	-1.3 (7)
Se1—C1—C6—H6	-2.9 (6)	H3—C3—C4—C5	-178.6 (7)
O1—C7—N1—C8	0.91 (12)	H3—C3—C4—H4	-0.1 (9)
O1—C7—C2—C1	178.42 (12)	C4—C3—C2—C7	179.69 (11)
O1—C7—C2—C3	-2.81 (13)	C4—C5—C6—H6	179.7 (6)
N1—Se1—C1—C2	-1.16 (6)	H4—C4—C5—C6	-177.6 (7)
N1—Se1—C1—C6	-179.23 (5)	H4—C4—C5—H5	0.2 (9)
N1—C7—C2—C1	-1.92 (10)	H5—C5—C6—H6	1.9 (9)
N1—C7—C2—C3	176.85 (11)	C6—C1—C2—C7	-179.70 (7)
N1—C8—C9—N2	179.05 (11)	C7—N1—C8—C9	-2.51 (11)
N1—C8—C9—H9	-0.2 (6)	C7—N1—C8—C12	177.56 (11)
N1—C8—C12—C11	179.83 (10)	C8—C9—N2—C10	1.76 (12)
N1—C8—C12—H12	0.1 (5)	C8—C12—C11—C10	0.48 (12)
N2—C10—C11—C12	0.23 (12)	C8—C12—C11—H11	180.0 (6)
N2—C10—C11—H11	-179.3 (6)	C9—N2—C10—C11	-1.35 (13)
N2—C9—C8—C12	-1.02 (12)	C9—N2—C10—H10	179.7 (5)
C1—Se1—N1—C7	0.13 (6)	C9—C8—C12—C11	-0.10 (13)
C1—Se1—N1—C8	179.76 (6)	C9—C8—C12—H12	-179.9 (5)
C1—C2—C3—C4	-1.58 (10)	H9—C9—N2—C10	-179.0 (8)
C1—C2—C3—H3	177.4 (6)	H9—C9—C8—C12	179.7 (8)
C1—C6—C5—C4	-0.92 (7)	C10—C11—C12—H12	-179.8 (5)
C1—C6—C5—H5	-178.7 (6)	H10—C10—C11—C12	179.2 (7)
C2—C1—C6—C5	-0.28 (10)	H10—C10—C11—H11	-0.3 (9)
C2—C1—C6—H6	179.1 (6)	H11—C11—C12—H12	-0.3 (9)

Hydrogen-bond geometry (Å, °)

<i>D</i> —H... <i>A</i>	<i>D</i> —H	H... <i>A</i>	<i>D</i> ... <i>A</i>	<i>D</i> —H... <i>A</i>
C9—H9...O1	1.08 (1)	2.09 (1)	2.772 (2)	119 (1)
C12—H12...Se1	1.08 (1)	2.58 (1)	3.1270 (12)	111 (1)
C6—H6...N2 <sup>i</sup>	1.08 (1)	2.41 (1)	3.0676 (18)	118 (1)
C6—H6...C9 <sup>i</sup>	1.08 (1)	2.61 (1)	3.3719 (16)	127 (1)
C12—H12...O1 <sup>ii</sup>	1.08 (1)	2.10 (1)	3.1262 (18)	158 (1)

Symmetry codes: (i)  $x-1/2, -y+3/2, z+1/2$ ; (ii)  $x+1/2, -y+3/2, z+1/2$ .